

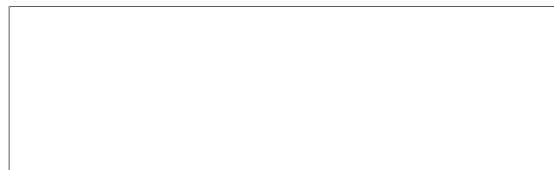
CONFIDENTIAL

H-2222-F

REF	7	REV	010580	BY	010956
WFO PROJ	033	REV	58	BY	50
WFO CLASS	M	REV	55	BY	C
WFO	22	REV	2010	BY	



25X1



25X1

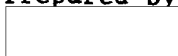
PHOTO GALVANIC CELL RESEARCH



25X1

FINAL REPORT

Prepared by



25X1

Period Covered: 1 May 1959 to 1 January 1960

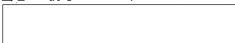
Report Date: 15 March 1960

CONFIDENTIAL



25X1

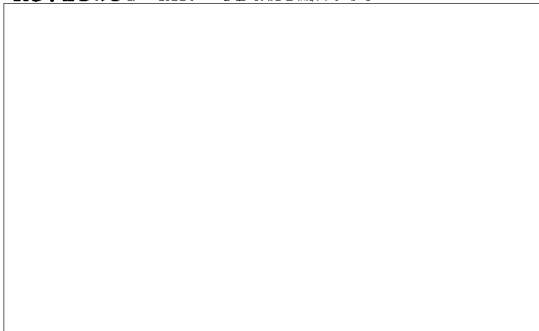
PREFACE

This is the Final Report pertaining to Photogalvanic Cell Research,  It concerns the progress made during the period 1 May 1959 to 1 January 1960.

25X1

This program was aimed at studying and developing electrolytic batteries which could operate normally without irradiation and be re-charged by light.

Reviewed and transmitted



25X1



TABLE OF CONTENTS

	Page
Preface	ii
List of Illustrations	iv
List of Tables	v
I. ABSTRACT	1
II. INTRODUCTION	1
III. PHOTOGALVANIC SILVER HALIDE BATTERIES	3
A. Silver Halide Membrane Type	3
B. Electrolytic Analogs of Semiconductor Junctions ...	11
C. Silver Halide Suspension Type	17
D. Discussion of Silver Halide Batteries	17
IV. PHOTOGALVANIC SEMICONDUCTOR BATTERIES	19
V. CONCLUSIONS	25
Appendix A: CYCLIC PHOTOGALVANIC SILVER HALIDE CELLS	26

LIST OF ILLUSTRATIONS

Figure	Title	Page
1	Schematic Illustrations of an Ag, AgCl, Aqueous FeCl ₂ FeCl ₃ (Pt) Photogalvanic Battery with Rectification Achieved by an Anion-Impermeable Membrane Combined with Complex Formation	4
2	Schematic Illustration of an Ag, AgCl, Aqueous FeCl ₂ FeCl ₃ (Pt) Photogalvanic Battery with Rectification Achieved by a Cation-Impermeable Membrane with a Three-Electrode Arrangement	5
3a	Design of Photogalvanic Cell with AgX Membrane	6
3b	Reaction Steps in AgX Photogalvanic Batteries	7
3c	Reaction Steps in AgX Photogalvanic Batteries	8
4	Comparison of Fixed and Mobile Charges in P-, N-, and I-type Semiconductors, Ion-Exchange Resins, and Water.....	12
5	Conceivable Semiconductor Junction Arrangements and Their Respective Electrolytic Analogs	14
6	Schematic Configurations of a P-N Semiconductor Diode with Ohmic Contacts, Its Electrolytic Analogs, and the Electrolytic Analog of a P-I-N Structure with Ohmic Contact	15
7	Schematic Configuration of an AgX Membrane Type Photogalvanic Cell with Rectification Achieved by an Electrolytic Analog of a P-I-N Junction	16
8	Combination of a Photovoltaic Diode with an Electrolytic Cell or with the Possible Circuit Equivalents of the Cell	20
9	Reversible Concentration Cell with Selectively Permeable Membrane	20
10	Electrolytic Resistance Cell	20



LIST OF ILLUSTRATIONS (cont'd)

Figure	Title	Page
11	Photogalvanic Semiconductor Cells without Charge Storage Capacity	23
12	Photogalvanic Semiconductor Cell with Charge Storage	24

LIST OF TABLES

Table	Title	Page
I	Comparison of Photochemical and Photogalvanic Quantum Yields in AgX Systems after Various Periods of Illumination by 30-Watt Tungsten Lamps with Reflecting Focusing Mirrors (Color Temperature 2600°K)	18

I. ABSTRACT

A basic chemical requirement for the operation of light-rechargeable batteries utilizing light-sensitive electrodes or separating membranes, is the presence in the electrolyte of an oxidation-reduction couple whose oxidation potential falls within a range determined by the oxidation-reduction potentials of the light-sensitive material and its photochemical products (cf. Eqs. (1) through (8), Section III). The chemical reaction steps that determine the performance of photogalvanic cells equipped with light-sensitive silver halide (AgX) membranes are given.

An improved performance may be expected for cells in which a suitable electrical space-charge field is created. Such a field could be formed either by an electrolytic analog of a semiconductor P-N junction (Section IV. B.) or by the formation of an actual P-N junction created by immersing a semiconductor in a suitable electrolyte (Section V). The latter method was shown to be effective in experiments with AgX and Ge. However, photogalvanic cells utilizing other light-sensitive semiconductors may also be improved by the methods developed during the present study (Section VI).

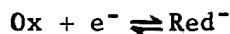
II. INTRODUCTION

The light-rechargeable batteries initially proposed operated in the manner described below.

Given a battery deriving its electromotive force E from the difference between the potentials E_1 and E_2 of the following half cell reactions:

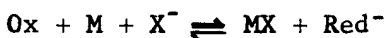


$$E_1 = E_1^0 - 0.059 \log (X^-) \quad (1)$$



$$E_2 = E_2^0 - 0.059 \log \frac{(Red^-)}{(Ox)} \quad (2)$$

so that the overall reaction on discharge is

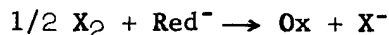


$$E = E_2 - E_1 \quad (3)$$

where MX is a light-sensitive, rather insoluble salt of a metal M (silver, copper, etc.) and a non-metal X (I, Br, Cl or O), Red⁻ and Ox are components of a suitable oxidation-reduction couple, and (X⁻), (Red⁻), (Ox) are the concentrations of the respective species in the aqueous electrolyte. Upon suitable irradiation of the light-sensitive discharge product MX, photolysis occurs:

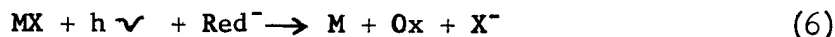


which will be accelerated if the X product is removed through the secondary reaction



$$E_3 = E_3^0 - 0.059 \log \frac{(\text{X}^-) (\text{Ox})}{(\text{Red}^-) (\text{X}_2)^{1/2}} \quad (5)$$

so that the overall resulting reaction, (4) + (5), is



which is the reverse of reaction (3); i.e., the battery is effectively recharged by light.

Reaction (5) can occur only if the potential E_3 is positive, which is tantamount to the condition that the potential E_4 for the reaction

$$1/2 \text{X}_2 + e^- \rightleftharpoons \text{X}^-$$

$$E_4 = E_4^0 - 0.059 \frac{(\text{X}^-)}{(\text{X}_2)^{1/2}} \quad (7)$$

be higher than E_2 . Furthermore, because reaction (3) must also yield a positive potential, it follows that

$$E_1 < E_2 < E_4 \quad (8)$$

25X1

This requirement imposes a basic limitation on the choice of a suitable oxidation-reduction couple.

AgX batteries, developed [] before the present contract came into effect, are shown in Figures 1 and 2. These, in turn, were improved by using light-sensitive, semipermeable membranes instead of light-sensitive electrodes (Figure 3a). The light sensitive membranes consisted of rolled single crystal or polycrystalline sheets of AgCl about 0.002" thick which could be partly converted on one side to AgBr or AgBr + AgI by exposure to a solution of HBr with or without HI.

25X1

Section IV.A.deals with the further study and development of the latter batteries, []

25X1

[] The developments presented in the subsequent sections (IV.B.,C.,D.;and V) occurred exclusively during the present contract.

25X1

III. PHOTOGALVANIC SILVER HALIDE BATTERIES

A. Silver Halide Membrane Type

The performance of photogalvanic cells, in which an AgX sheet acts both as the basic light-sensitive material and as a semipermeable membrane for the separation and storage of the photochemical reaction products, is formulated in the following steps and is shown schematically in Figures 3b and 3c:

Photochemical Charging (Figure 3b)

1. $h\nu \rightarrow e^- + h^+$
2. $e^- + Ag^+ \text{ (in AgX)} \rightarrow Ag \text{ (in AgX)}$
3. $h^+ \text{ (in AgX)} \rightarrow h^+ \text{ (at AgX-electrolyte}_I \text{ interface)}$
4. $Ag^+ \text{ (at AgX-electrolyte}_I \text{ interface)} \rightarrow$
 $Ag^+ \text{ (at AgX-electrolyte}_{II} \text{ interface)}$
5. $h^+ + X^- \rightarrow 1/2 X_2 \text{ (at AgX-electrolyte}_I \text{ interface)}$ where e^-
and h^+ are free electrons and holes, respectively.
6. $1/2 X_2 + Red_I + Ag^+ \rightarrow Ox_I^+ + AgX$
7. $Ox_I^+ \text{ (at AgX-electrolyte}_I \text{ interface)} \rightarrow$
 $Ox_I^+ \text{ (at Pt}_I \text{ electrode)}$

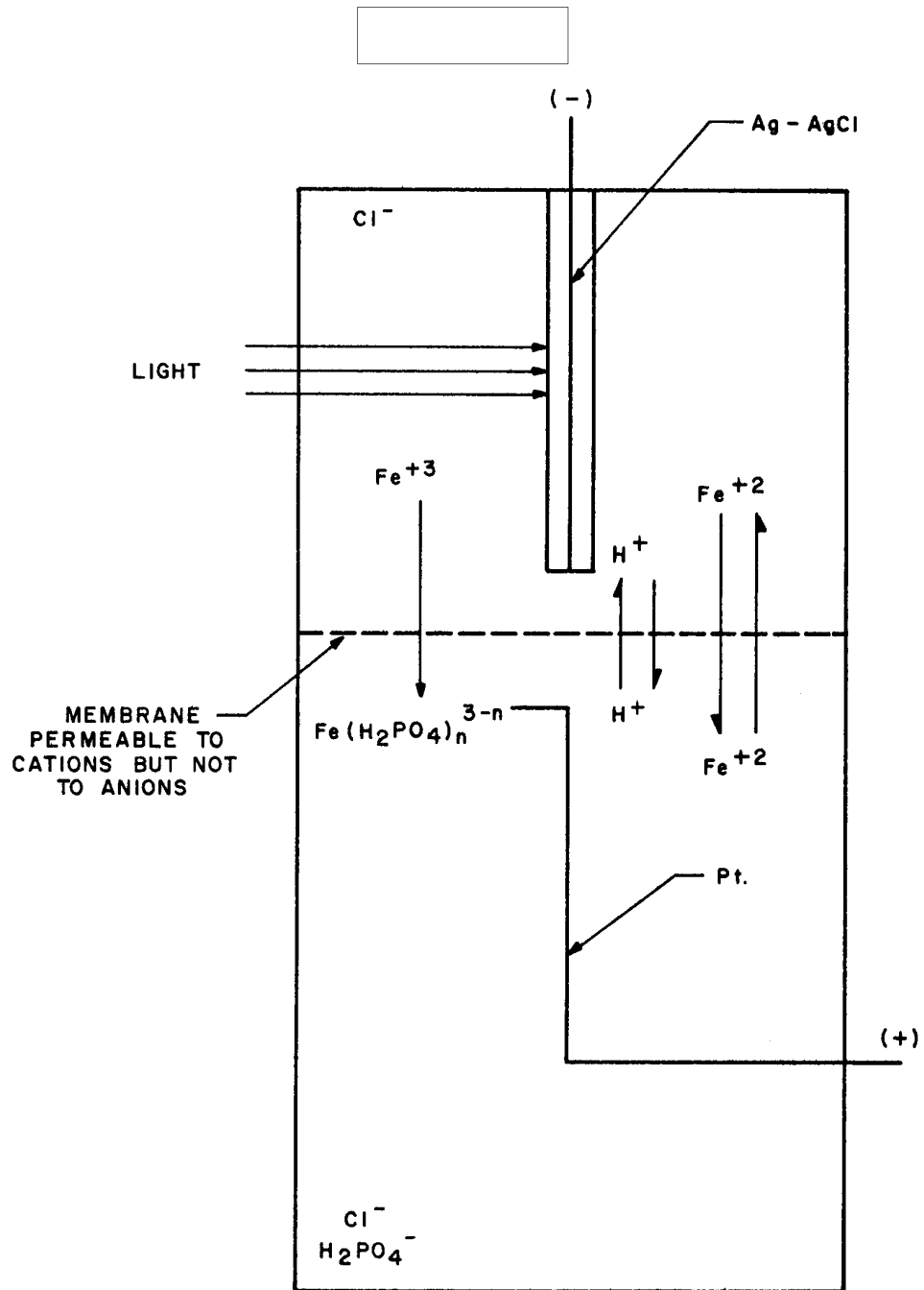
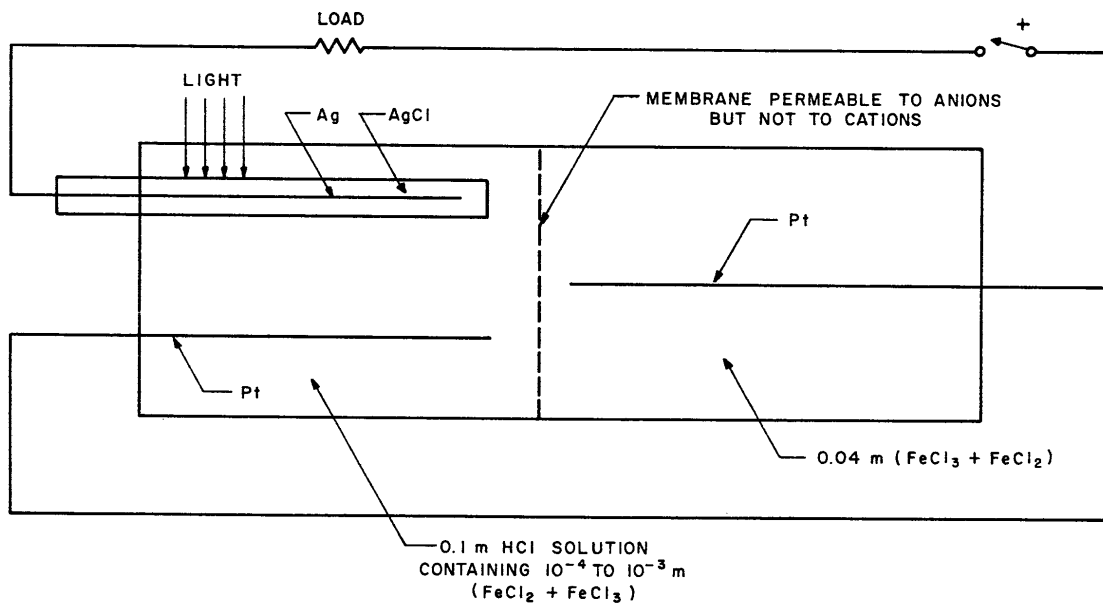


FIGURE 1 SCHEMATIC ILLUSTRATION OF AN $\text{Ag, AgCl, AQUEOUS FeCl}_2 \parallel \text{FeCl}_3 (\text{Pt})$ PHOTO GALVANIC BATTERY WITH RECTIFICATION ACHIEVED BY AN ANION-IMPERMEABLE MEMBRANE COMBINED WITH COMPLEX FORMATION



- 5 -

25X1

FIGURE 2 SCHEMATIC ILLUSTRATION OF AN Ag, AgCl, AQUEOUS $\text{FeCl}_2 || \text{FeCl}_3$ (Pt) PHOTO GALVANIC BATTERY WITH RECTIFICATION ACHIEVED BY A CATION- IMPERMEABLE MEMBRANE WITH A THREE - ELECTRODE ARRANGEMENT

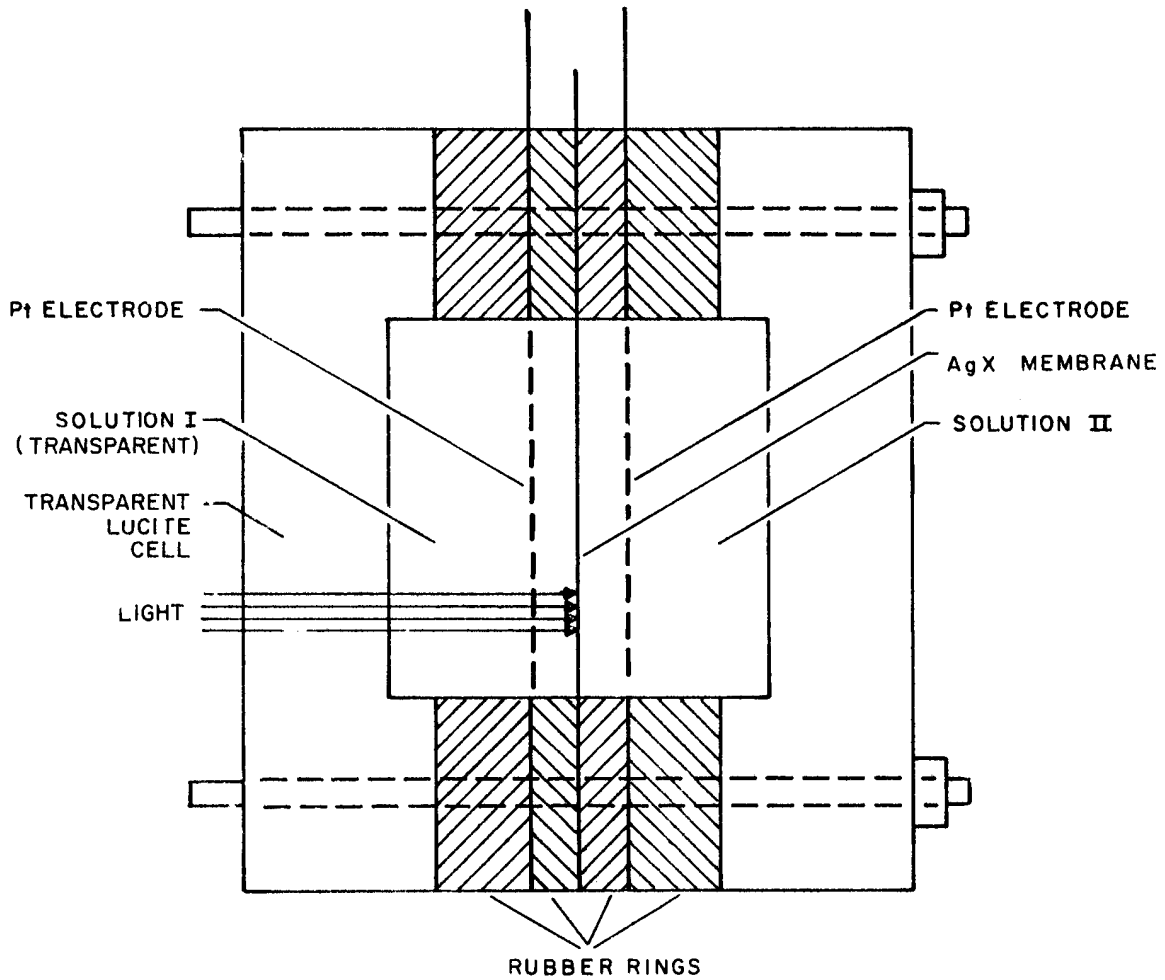


FIGURE 3a DESIGN OF PHOTOGALVANIC CELL WITH AgX MEMBRANE

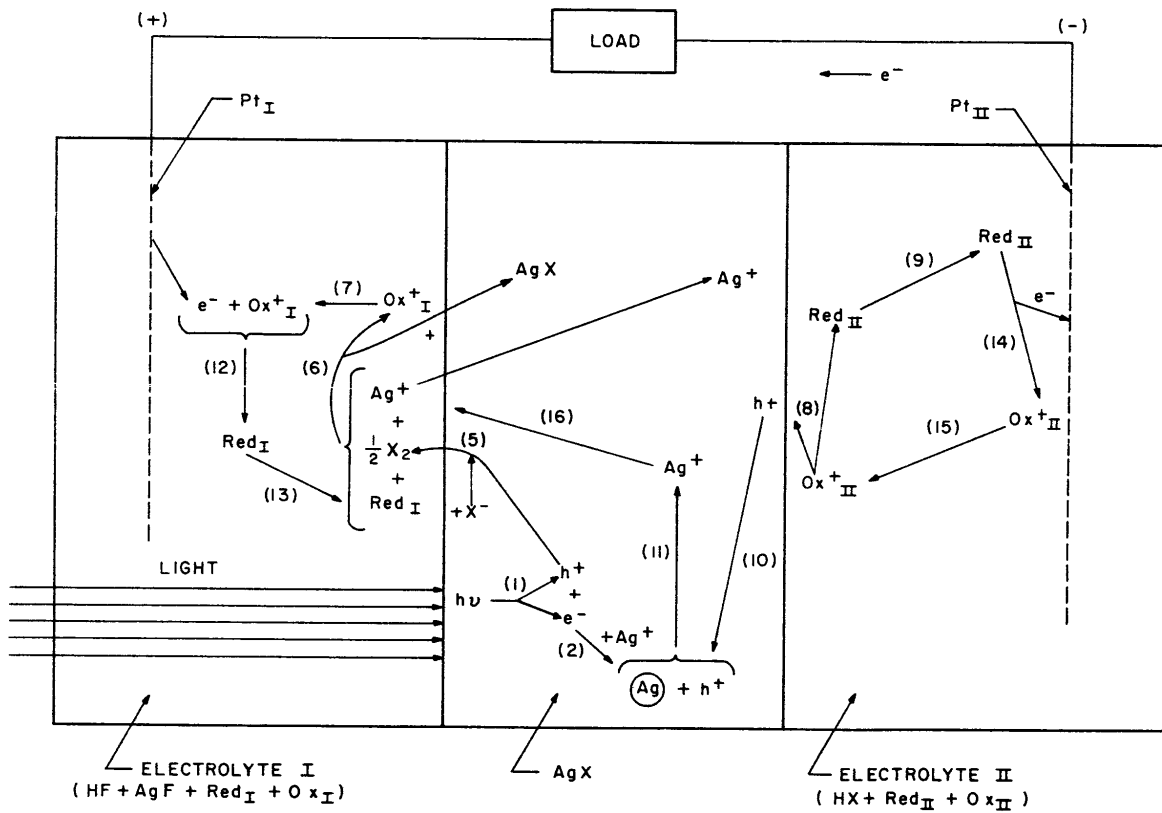
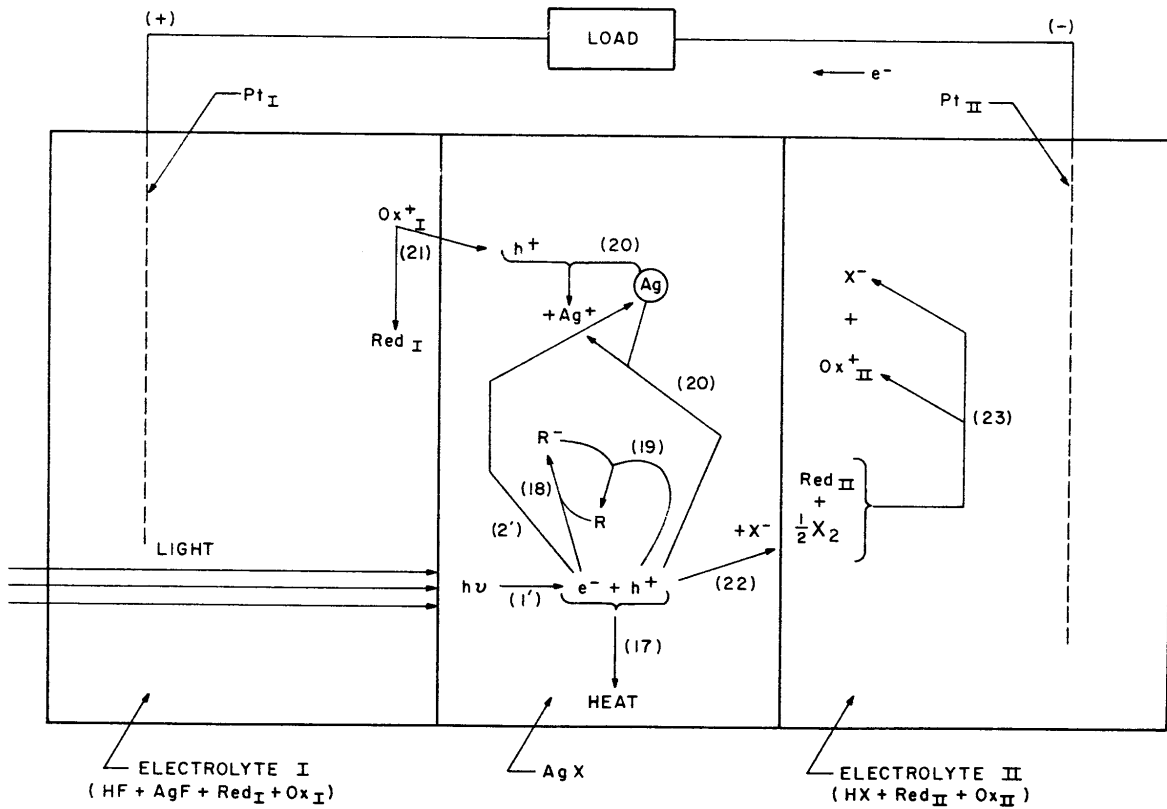


FIGURE 3b REACTION STEPS IN AgX PHOTOGALVANIC BATTERIES

- 8 -



25X1

FIGURE 3c REACTION STEPS IN AgX PHOTO GALVANIC BATTERIES



8. Ox_{II}^+ (at AgX-electrolyte_{II} interface) \longrightarrow
 h^+ + Red_{II} (at AgX-electrolyte_{II} interface)
9. Red_{II} (at AgX-electrolyte_{II} interface) \longrightarrow Red_{II} (at Pt_{II})
10. h^+ (at AgX-electrolyte_{II} interface) \longrightarrow h^+ (at Ag in AgX)
11. h^+ + $\text{Ag} \longrightarrow \text{Ag}^+$ (in AgX)

Discharge through a Load (Figure 3b)

12. $\text{Ox}_{\text{I}}^+ + \text{e}^- \longrightarrow \text{Red}_{\text{I}}$ (at Pt_I electrode)
13. Red_{I} (at Pt_I) \longrightarrow Red_{I} (at AgX-electrolyte_I interface)
14. $\text{Red}_{\text{II}} \longrightarrow \text{Ox}_{\text{III}}^+ + \text{e}^-$ (at Pt_{II} electrode)
15. Ox_{II}^+ (at Pt_{II}) \longrightarrow Ox_{II}^+ (at AgX-electrolyte_{II} interface)
16. Ag^+ (at AgX-electrolyte_{II} interface) \longrightarrow
 Ag^+ (at AgX-electrolyte_I interface)

Undesirable Competing Reactions (Figure 3c)

17. $\text{e}^- + \text{h}^+ \longrightarrow \text{heat}$
18. $\text{e}^- + \text{R} \longrightarrow \text{R}^-$
19. $\text{R}^- + \text{h}^+ \longrightarrow \text{R}$ (where R, R⁻ may be an impurity or lattice defect acting as a center for the recombination of holes with electrons)
20. $\text{h}^+ + \text{Ag} \longrightarrow \text{Ag}^+$
21. Ox_{I}^+ (at AgX-electrolyte_I interface) \longrightarrow h^+ + Red_{I}
22. $\text{h}^+ + \text{X}^- \longrightarrow 1/2 \text{X}_2$ (at AgX-electrolyte_{II} interface)
23. $1/2 \text{X}_2$ (at AgX-electrolyte_{II} interface) X $\text{Red}_{\text{II}} \longrightarrow \text{X}^- + \text{Ox}_{\text{II}}^+$

□

Steps (17) and/or (18) - (19) and/or (20) compete with steps (2) and (3). Step (21) competes with steps (6) through (10), and steps (22) - (23) compete with steps (5) through (15). The difference between steps (20) and (11) is that in the latter step, the positive hole had originated at the AgX-solution II interface (step (8)).

The charging and useful discharging reaction steps (1) through (3), and (5) through (16) involve the motion of positive charges from Pt_{II} through electrolyte II through the AgX towards electrolyte I and Pt_I, whereas the competing parasitic reactions involve charge motion in the opposite direction, steps (20) through (22); or in either direction, steps (17) through (19). Step (17) is of minor importance except under conditions of intense illumination. Hence, in the absence of the recombination centers R, the main problem would consist in favoring steps (1) through (16) and obviating steps (20) through (23).

An electric field within the AgX favoring the motion of positive charges from right to left should tend to obviate the undesirable steps (20) through (23) and favor all but one of the desired steps (1) through (16). The one exception is the charging step (4) which would have to proceed against the direction of the field. However, when charge is withdrawn as the cell is illuminated (which occurred in most of the experiments) the discharging step (16) should cancel step (4), since these two steps are equal and opposite in direction. Therefore, under these conditions the proposed field should lead to improved yields. Two alternate methods of achieving this field without applying an auxiliary external voltage are discussed in Sections IV. B. and V.

B. Electrolytic Analogs of Semiconductor Junctions

It is known that space-charge regions exist in electrolytes near metal electrodes, precipitated particles (Helmholtz and Gouy type layers), and selectively permeable ion-exchange membranes. The latter resemble semiconductors to the extent that they contain immobile species of one charge sign and mobile species of an opposite sign.

The mobile H_3O^+ and OH^- ions in aqueous solutions and ion-exchange membranes are analogs of the holes, h^+ , and electrons e^- , while the immobile anionic and cationic groups in ion-exchange membranes resemble the acceptors and donors in semiconductors.

The recombination of holes and electrons giving rise to the equilibrium condition in semiconductors

$$(e^-) (h^+) = K_s \quad (9)$$

is analogous to the acid-base neutralization equilibrium

$$(OH^-) (H_3O^+) = K_w \quad (10)$$

and also to the precipitation equilibrium for insoluble salts such as AgX

$$(Ag^+) (X^-) = K_{AgX} \quad (11)$$

where the symbols in parentheses are the concentrations of the respective species. Because the constants K_s , K_w and K_{AgX} are of the order of $10^{-13 \pm 3}$ (millimoles/cc)² both in water and in good semiconductors, Equations (9) and (10) afford a means of reducing the concentration of the mobile species of any one charge sign to an extremely low value, thus providing the basis for good rectification. However, if other highly mobile ionic species Y^+ and Z^- , e.g., Na^+ and/or NO_3^- ions, which are not subject to recombination, are also present in solution, then the product of oppositely charged carrier concentrations may become much larger than K_w . The aqueous solution would then be equivalent to a semiconductor with a high value of K_s , i.e., a "low band-gap" semiconductor with rather poor rectifying ability. Finally, when the concentration of mobile Y^+ and Z^- ions exceeds 0.1 M, the aqueous solution becomes equivalent to a highly conductive "degenerate" semiconductor with no appreciable rectifying ability.

When the concentrations of Y^+ and Z^- ions are less than 0.1 M, Figure 4 shows the analogy between semiconductors containing an excess of

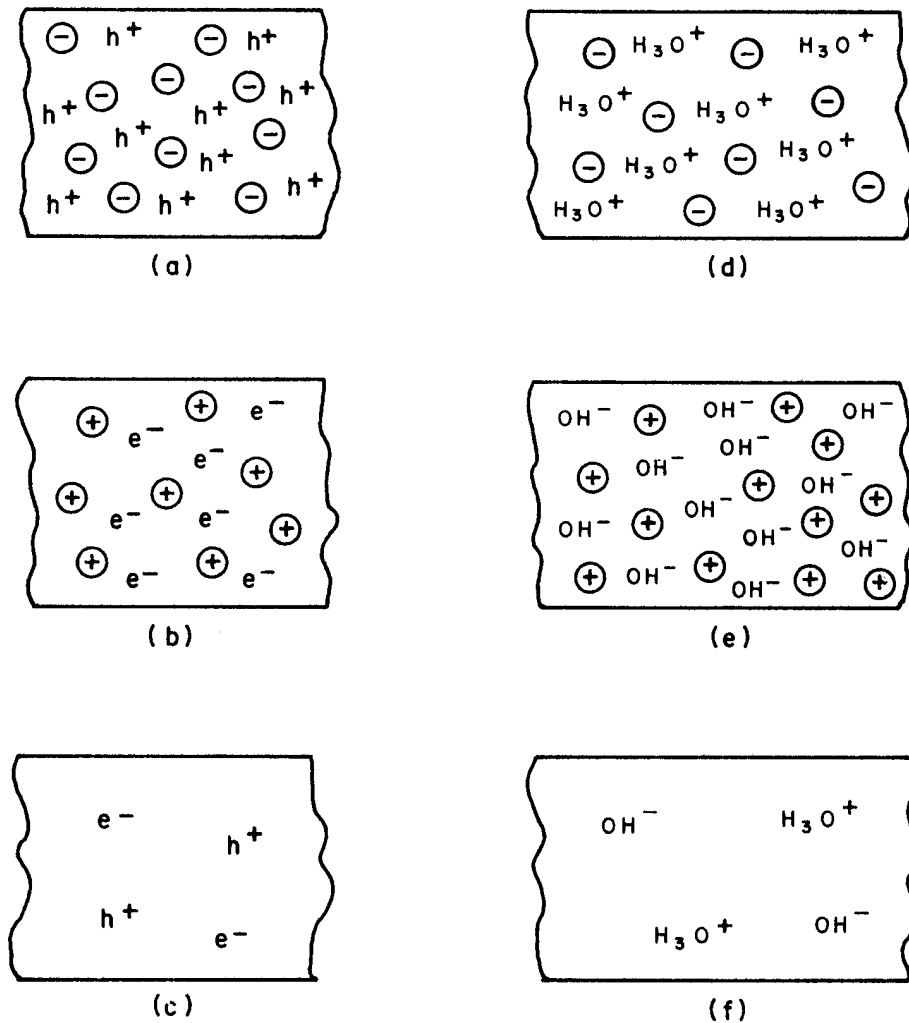


FIGURE 4 COMPARISON OF FIXED (ENCIRCLED) AND MOBILE CHARGES IN P-, N-, AND I-TYPE SEMICONDUCTORS (a), (b), AND (c), RESPECTIVELY, AND ION-EXCHANGE RESINS (d) AND (e), AND WATER (f). THE RIGHT-HAND DIAGRAMS ARE ELECTROLYTIC ANALOGS OF THE ADJACENT SEMICONDUCTOR TYPES.

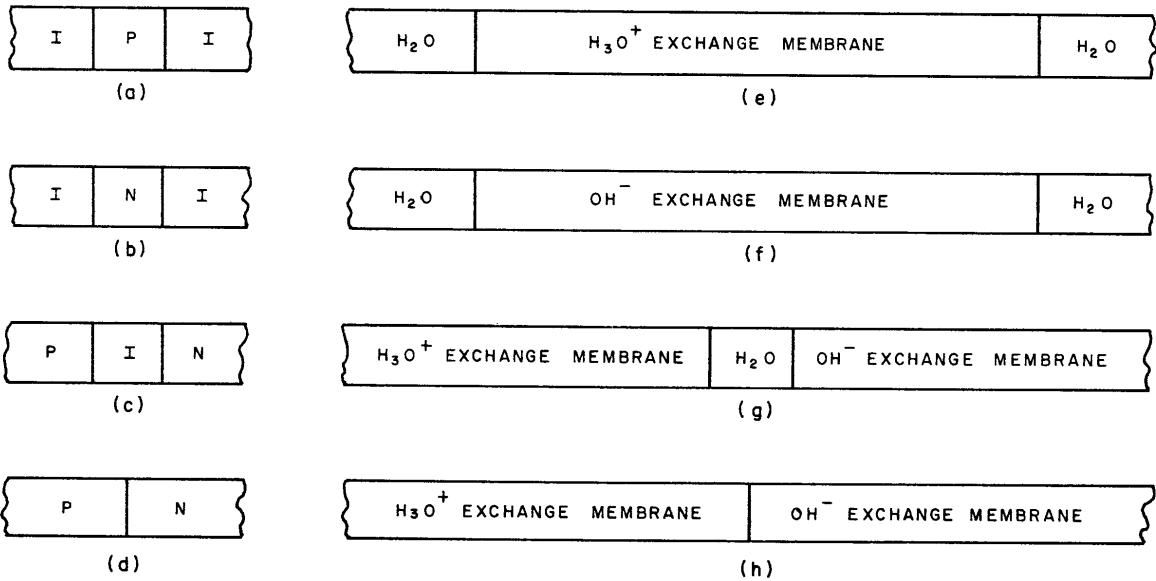
holes (p-type), electrons (n-type) or neither (intrinsic or n-type), on the one hand, and aqueous solutions or resins containing an excess of H_3O^+ ions, OH^- ions, or neither (pure water), on the other hand.

Figure 4 demonstrates the possibility of obtaining an electrolytic analog of every conceivable type of semiconductor junction, simply by arranging the corresponding components in corresponding order, as shown in Figure 5. Of the eight diagrams of Figure 5, only (c), (d), (e) and (f) are currently used. The I-P-I and I-N-I arrangements, (a) and (b), do not seem to offer useful applications in semiconductor technology; however, their electrolytic analogs (e) and (f), are the only arrangements in which ion-exchange membranes have been extensively used thus far. Nevertheless, because the P-I-N and P-N arrangements (c) and (d) are known to have excellent rectifying characteristics, it is worthwhile to examine their electrolytic analogs (g) and (h) more closely.

Arrangements (g) and (h) of Figure 5 require electrical contacts to the end regions similar to the "ohmic" contacts of the p- and n-type semiconductor regions required for the utilization of a diode in an external circuit. Of course, reversible half cell electrodes with fairly concentrated electrolytes would form the equivalent of an ohmic contact as long as the concentrated electrolytes remain only on one side of each membrane, as shown in Figures 6a and 6b. However, the concentrated electrolytes composed of small ions would rapidly permeate the membranes, and destroy all the junctions. Fortunately, it is possible to use highly soluble large sized ions impermeable through the membranes, e.g., long-chain organic quaternary ammonium or sulfonate ions. This system is indicated in Figures 6c and 6d, which represent the practical electrolytic analogs of semiconductor P-N and P-I-N diodes.

As long as the membranes shown in Figures 6c and 6d remain impermeable to the long-chain ions, the reversible reduction-oxidation couples, composed of ions of the type Y^+ and Z^- should remain separated for an indefinitely long time. Thus, it is theoretically possible to construct rechargeable inert-electrode batteries with reactants stored indefinitely in adjacent aqueous solutions.

An application of arrangements analogous to those of Figures 6c and 6d is shown in Figure 7, which represents an improved model of an AgX cell of the Figure 3 type. The latter cell yielded the highest currents with very thin sheets of AgX. However, the thin sheets readily developed pores and caused the mixing of the electrolytes. Because the arrangement of Figure 7 provides for a permanent separation of the two electrolytic solutions, extremely thin AgX sheets may be employed.



- 14 -

25X1

FIGURE 5 CONCEIVABLE SEMICONDUCTOR JUNCTION ARRANGEMENTS (a), (b), (c), AND (d) AND THEIR RESPECTIVE ELECTROLYTIC ANALOGS (e), (f), (g), AND (h)

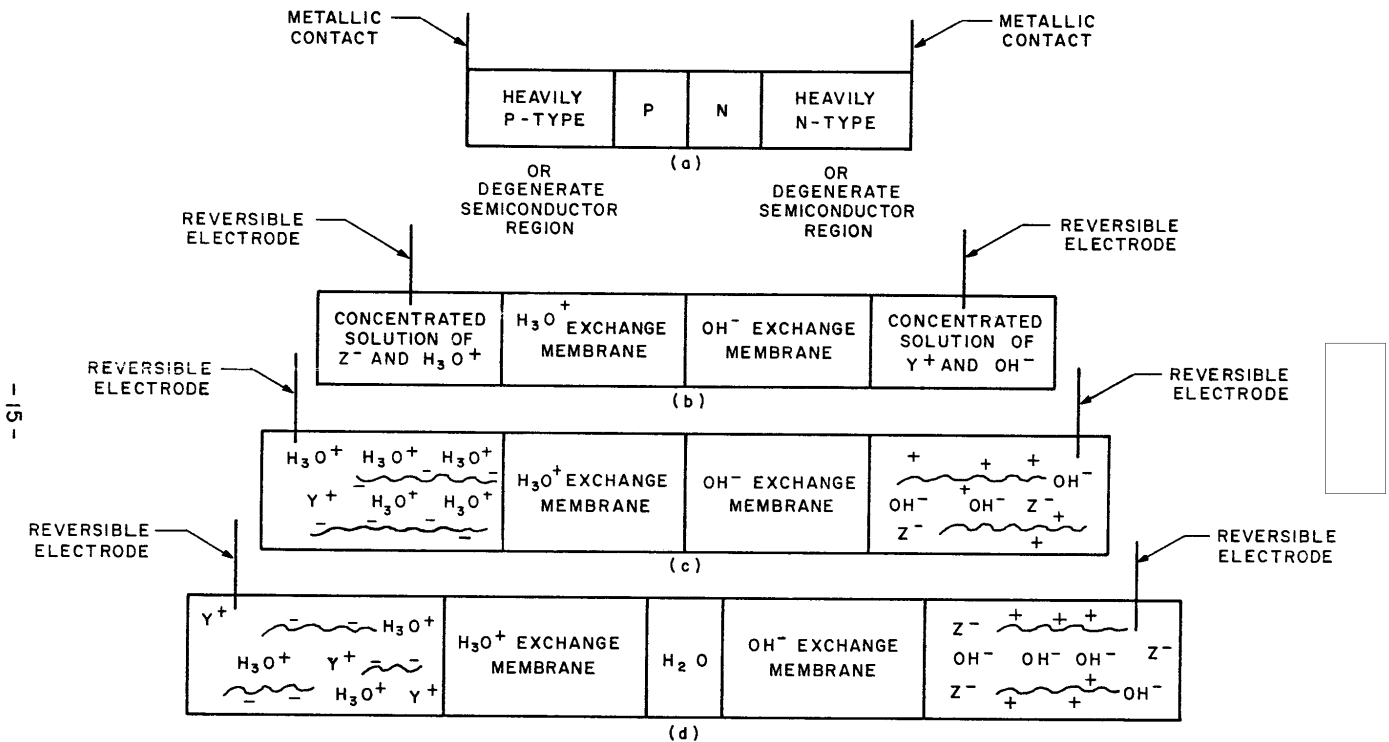


FIGURE 6 SCHEMATIC CONFIGURATIONS OF A P-N SEMICONDUCTOR DIODE WITH OHMIC CONTACTS (a), ITS ELECTROLYTIC ANALOGS (b) AND (c), AND THE ELECTROLYTIC ANALOG OF A P-I-N STRUCTURE WITH OHMIC CONTACTS (d). DIAGRAM (b) REPRESENTS A TRANSIENT CONFIGURATION. DIAGRAMS (c) AND (d) REPRESENT CONFIGURATIONS STABILIZED BY LONG-CHAIN IONS.

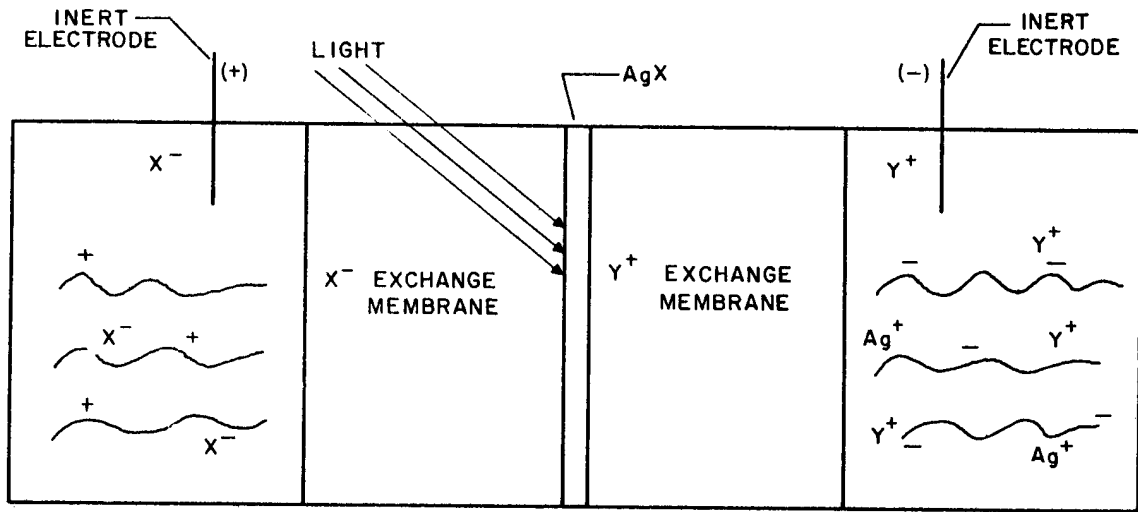



FIGURE 7 SCHEMATIC CONFIGURATION OF AN AgX MEMBRANE TYPE PHOTO GALVANIC CELL WITH RECTIFICATION ACHIEVED BY AN ELECTROLYTIC ANALOG OF A P-I-N JUNCTION



Reaction between photolytic halogen and the ion-exchange membranes adjacent to the illuminated AgX had to be prevented in the cell of Figure 7. This reaction was prevented by an exhaustive bromination process which, unfortunately, also rendered the initially transparent membranes opaque to blue light. However, it should be possible to prepare transparent exhaustively chlorinated or fluorinated ion-exchange membranes suitable for the arrangement of Figure 7.

C. Silver Halide Suspension Type

Two 15 cc compartments separated by an anion exchange membrane, each containing a Pt electrode, were filled with the same solution of 0.005 M FeSO_4 plus 0.5 M H_2SO_4 . One compartment also contained 10 gms of fine AgBr particles and a small glass-encapsulated stirring magnet. The compartments, once filled and closed, were placed in the dark and allowed to equilibrate overnight. Subsequently, the solution containing AgBr was continuously illuminated with a 30-watt microscope lamp and stirred. A flow of electric current through a 50-ohm load began immediately. The current climbed slowly to a maximum value of 1.5 ma within 2 hours and remained in the range of 1 to 1.5 ma for more than 3 hours. The quantum yield was 20% to 50%.

Two objectionable features of this type of cell were: (a) stirring was required for maximum current output; (b) the cell was essentially a concentration cell, hence the voltage output was neither likely to reach nor appreciably exceed the value of 0.1 v; and even such a low value could not be maintained for a long period of time. Nevertheless, the initial current yields with these cells bridge the gap between the high photochemical quantum yields (50% to 100%) obtained for periods of several hours with stirred AgX powders (and for the first five minutes of illumination with AgX sheets), and the relatively low photogalvanic quantum yields (1% to 5%) obtained with AgX electrodes and membranes for periods of several days. See Table I.

D. Discussion of Silver Halide Batteries

In Table I the photogalvanic quantum yields obtained with the three types of AgX cells described in Sections III and IV are compared with measured photochemical quantum yields.

In AgX membrane type cells, photochemical yields decreased rapidly upon prolonged illumination because Ag accumulated near the AgX surface. This explanation was confirmed by etching down the surface of previously illuminated AgX sheets; the etched sheets gave initial photochemical quantum yields comparable to those of freshly illuminated,

TABLE I

Comparison of Photochemical and Photogalvanic Quantum Yields in AgX Systems after Various Periods of Illumination by 30-Watt Tungsten Lamps with Reflecting Focusing Mirrors (Color Temperature 2600°K)*

SYSTEMS	QUANTUM YIELDS AFTER ILLUMINATION TIME OF:				
	0-5 min.	5 min. to 3 hrs.	3 hrs. to 1 day	1 day to 1 wk.	> 1 week
a. Photochemical:					
Stirred AgCl and AgBr powders	50-100%	50-100%	10-50%	---	---
AgCl and AgBr sheets	50-100%	negligibly low	---	---	---
b. Photogalvanic Cells					
Cells with AgX membranes	---	1-2%	1-2%	≈ 1%	≈ 1%
Cells with AgX electrodes	1-5%	1-5%	1-3%	0-2%	0
Cells with AgBr in suspension	---	20-50%	1-10%	0	0

* In computing the quantum yields, only the light of wavelengths shorter than the absorption edge of the AgX was considered.

previously unexposed sheets. The ability of AgX membrane type cells to deliver appreciable currents for periods of several weeks, suggests that Ag accumulation is somewhat reduced by a regeneration mechanism of the kind shown in Figure 3b.

Excessive surface accumulation of Ag was probably the main cause of deterioration in AgBr suspension type cells and at least a partial cause of deterioration in the other cell types.

AgX electrode cells, which did not contain solid Ag initially, deteriorated in less than 1 week partly because of the formation of pores.

Although batteries with solid Ag electrodes delivered appreciable current for much longer periods of time, the true photogalvanic quantum yields could not be measured easily (see Appendix A, Section I. A.).

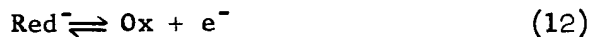
Initial maximum photogalvanic quantum yields were higher for the poorer cells (AgBr in suspension) and lower for the cells with AgX membranes. The reverse was true when total photogalvanic currents were computed over a period of more than 1 week: the AgX membrane cells supplied the larger amounts of total charge upon prolonged illumination.

Most of the cells tested were composed of solid AgCl sheets covered with AgBr-AgI on the illuminated side, containing 1 M HCl in the illuminated compartment, and 0.01 to 0.1 M FeSO₄ (with or without 0.01 M Ag₂SO₄) in 0.5 M H₂SO₄ (or saturated CuCl in 1M HCl) in the dark compartment.

The potentialities of the AgX cells are still inadequately explored. In addition to the large variety of available membranes, long-chain ions, and oxidation-reduction couples having suitable electrode potentials, there are reasons to experiment with (a) the AgX thicknesses and the ratios of AgBr to AgI for maximum light-sensitivity and ionic mobility, and (b) the inclusion of impurities for extending the wavelength spectrum of the useful radiation, improving ionic mobilities, and removing or neutralizing harmful recombination centers.

IV. PHOTOGALVANIC SEMICONDUCTOR BATTERIES

Before examining photogalvanic semiconductor cells, it is convenient to consider the circuits of Figure 8. Electrolytic cell (a) of Figure 8 may be of the form shown in Figures 9 and 10. It is composed mainly of two inert electrodes immersed in an electrolytic solution containing reversibly oxidizable and reducible ions, Red⁻ and Ox, such that the reaction



can occur at either one of the electrodes at appreciable current densities. The electrolyte composition is initially uniform throughout the cell. When switch 1 is closed, cell (a) at first behaves like a purely resistive element, as represented by the equivalent circuit (b) with switch 2 closed. Reaction (1) will then proceed from left to right at one inert electrode and from right to left at the other. This will produce local changes in the concentrations of Red⁻ and Ox with continued passage of photovoltaic current through the cell.

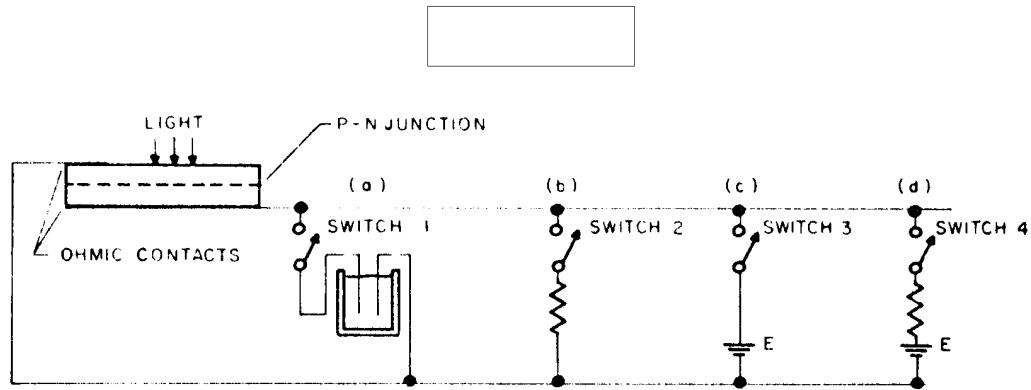


FIGURE 8 COMBINATION OF A PHOTOVOLTAIC DIODE WITH AN ELECTROLYTIC CELL (a) OR WITH THE POSSIBLE CIRCUIT EQUIVALENTS OF (a)

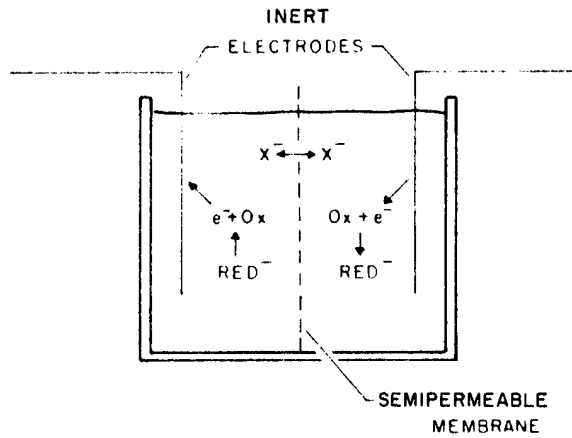


FIGURE 9 REVERSIBLE CONCENTRATION CELL WITH SELECTIVELY PERMEABLE MEMBRANE

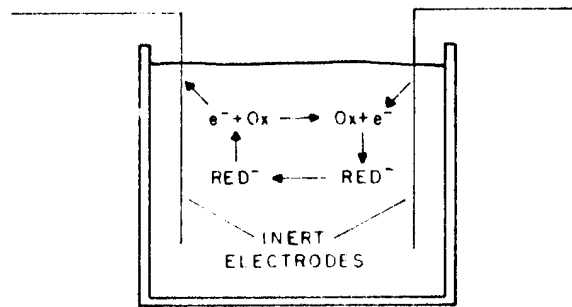


FIGURE 10 ELECTROLYTIC RESISTANCE CELL



In the cell of Figure 9, these local concentration changes are tantamount to the charging of a concentration cell. The cell is therefore equivalent to circuit element (c) or (d) of Figure 8 with switch 3 or 4 closed. The charging can then continue only until the counter-voltage built up in the cell is equal to the maximum photo-voltage of the illuminated diode. However, if the semipermeable membrane is eliminated, as shown in Figure 10, then mixing occurs and the concentration cell counter-voltage is reduced. A steady state is reached when the electrode reaction products are carried away as fast as they are formed, by convection currents, diffusion, and by electric fields. The cell is then still equivalent to circuit element (d) of Figure 8, but with a low value of the counter-voltage E . Finally, if the concentrations of the Ox and Red^- components are high and the electrodes almost adjacent, the counter-voltage E may become negligibly low and the cell may be considered nearly equivalent to the purely resistive element (b).

A simplification of the arrangement of Figure 1 would be achieved:

- (a) if a semiconductor electrode behaved like an inert electrode when immersed in the electrolyte of cell (a) and
- (b) if the electrolyte changed the conductivity type of the region of the semiconductor so as to form a P-N type junction therein.

It is known that an electrolyte can form a p-type layer over an n-type semiconductor or an n-type layer over a p-type material by forming a surface layer of ions of the same charge sign as the majority carrier in the semiconductor.¹ This layer of ions is formed either by preferential adsorption of certain ions which have a specific affinity for the semiconductor surface, or by an electrochemical potential gradient across the semiconductor-electrolyte interface favoring the displacement of ions of one charge sign towards the semiconductor surface.^{2,3}

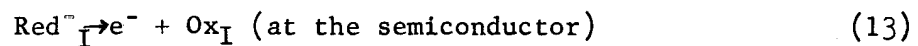
Since illumination of a semiconductor P-N junction is known to yield excellent photovoltaic effects, illumination of an electrolyte-induced P-N junction should also generate marked photogalvanic currents.

-
1. W. H. Brattain and C. G. B. Garrett, "Electrical Properties of the Interface Between a Germanium Single Crystal and an Electrolyte," PHYSICAL REVIEW, Vol. 94, No. 3, May 1954, p. 750.
 2. Ibid.
 3. W. H. Brattain and C. G. B. Garrett, U. S. Patent No. 1,870,344, p. 3, lines 50 to 75.

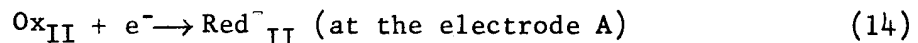
Cells based on this phenomenon are shown in Figures 11 and 12.

When the above requirements (a) and (b) are met, the cells of Figures 11 and 12 become equivalent to the arrangement of Figure 8a. The electrolytic cells of Figure 11 resemble that of Figure 10, while the cell of Figure 12 is analogous to that of Figure 9, in allowing for charge storage. In Figure 11a part of the light is absorbed by the electrolyte solution which must therefore be free of appreciable concentrations of light-absorbing ions. This limitation is by-passed in the arrangement of Figure 11b where the light may pass through a transparent ohmic contact. Such a contact will be even more useful in the cell of Figure 12. The latter cell operates as described below.

Upon illumination, the photovoltaic flow of electrons through the solution, the separating membranes, electrode A, diode D, and the semiconductor, results in the charging reactions



and



On discharge through a load, the reverse reactions can then occur at electrodes C and B, respectively. The diode D (which may not be needed in some systems) prevents discharge through the photovoltaic charging circuit in the dark.

A variation of Figure 11b is shown in Figure 3a where the transparent ohmic contact consists of a second electrolyte solution which tends to induce the same conductivity type to the AgX surface as that of the original bulk material.

Cells of the Figure 11a type actually yielded appreciable photogalvanic currents with:

- (a) n-type AgCl or AgBr as semiconductor electrode, Ag or Pt as the ohmic contact, $\text{Fe}^{+2} - \text{Fe}^{+3}$ as the $\text{Red}^- - \text{Ox}$ couple, and Cl^- or Br^- as the adsorbed ions inducing p-type conductivity to the AgX surface; and
- (b) p-type Ge as semiconductor and $\text{Ti}^{+2} - \text{Ti}^{+3}$ and/or $\text{Cr}^{+2} - \text{Cr}^{+3}$ as the $\text{Red}^- - \text{Ox}$ couples.

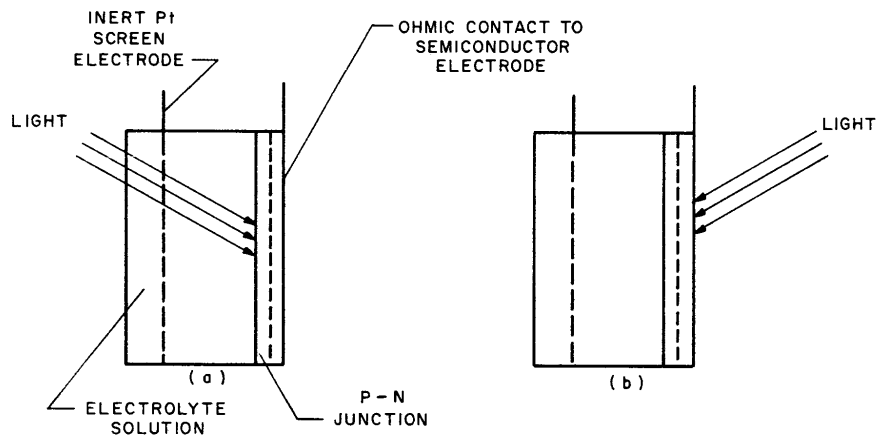
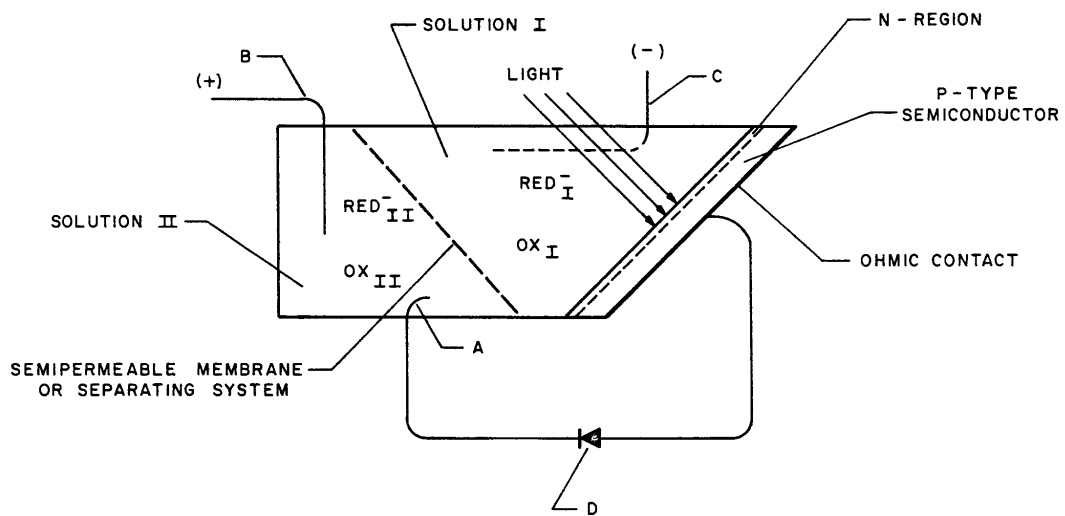


FIGURE II PHOTOGALVANIC SEMICONDUCTOR CELLS WITHOUT CHARGE STORAGE CAPACITY. (a) LIGHT MUST PASS THROUGH THE ELECTROLYTE SOLUTION BEFORE REACHING THE SEMICONDUCTOR. (b) LIGHT CAN PASS THROUGH A TRANSPARENT CONDUCTOR FORMING AN OHMIC CONTACT TO AN EVAPORATED SEMICONDUCTOR FILM.



25X1

FIGURE 12 PHOTOGALVANIC SEMICONDUCTOR CELL DESIGN

A typical electrolyte solution in the latter cell type was composed of 0.0015 M GeCl_4 + 0.05 M NaCl + 0.01 M HCl + 0.15 M (TiCl_2 + TiCl_3) + 0.5 M (CrCl_3 + CrCl_2). Photogalvanic currents of 10-100 μA have already been obtained with such cells upon relatively weak illumination, but much more study will be required to optimize the yields from these cells.

V. CONCLUSIONS

A basic chemical requirement for the operation of light-rechargeable batteries utilizing light-sensitive electrodes or separating membranes, is the presence in the electrolyte of an oxidation-reduction couple whose oxidation potential falls within a range determined by the oxidation-reduction potentials of the light-sensitive material and its photochemical products (cf. Eqs. (1) through (8), Section III.A.).

Although the light-responsive substances studied were mainly AgX and Ge, the designs shown in Figures 1 to 3, 7, 11, and 12, as well as the relevant basic theory, should be applicable to other photogalvanic systems. Furthermore, the possibility of photogalvanic effects arising from a combination of a semiconductor P-N junction photovoltaic effect and regular electrode behavior has been at least partly confirmed by the experiments with Ge and AgX types of cells.

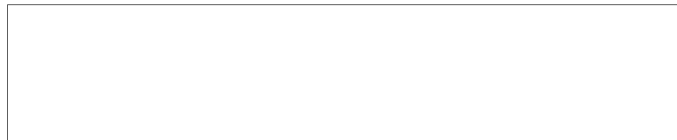
Since the operation of the AgX type photogalvanic cells also appears to be related to a P-N junction photovoltaic diode effect, the established theory of this effect appears applicable. Now, the optimum theoretical efficiency for the conversion of solar radiation into electricity is obtainable with semiconductors having a 1.5 e.v. intrinsic band-gap width, which is less than half the width of the silver halides (3 to 4 e.v.). Therefore, it appears desirable to investigate photogalvanic systems utilizing semiconductors with an optimum band-gap width.

This program has augmented the theoretical and technical knowledge of photogalvanic phenomena; however, there were many barriers to development of an efficient photogalvanic cell. For example, in the AgX membrane type cells, Ag accumulated near the AgX surface and photochemical yields decreased substantially upon prolonged illumination. In the AgX suspension type cells, excessive accumulation of Ag caused deterioration of the cells; voltage output was low and could not be maintained long. Cell deterioration was also encountered in the AgX electrode type cells. These deteriorated, partially because of the formation of pores.

Because of these difficulties and the additional experimentation yet required in associated areas, continued research activity with an efficient photogalvanic cell as its end product would not be practical at this time.

APPENDIX A

CYCLIC PHOTOGALVANIC SILVER HALIDE CELLS



25X1

Cyclic Photogalvanic Silver Halide Cells

25X1

ABSTRACT

In order to distinguish between photoconductive or photocatalytic and "truly photogalvanic" effects, continuous photocurrent measurements were performed on cyclic Pt, Ag - AgCl, aqueous FeCl₂ - FeCl₃, Pt and Pt, Ag - AgBr, aqueous FeBr₂ - FeBr₃, Pt batteries in a state of nearly complete discharge. These batteries could be partly recharged by light of wavelengths shorter than 4300 Å and 4800 Å, respectively, with maximum photogalvanic quantum yields of 2 to 5%. These quantum yields vary mainly with method of electrode preparation, electrolyte composition, and light wavelength, but not with light intensity for intensities equivalent to usual solar radiation levels. Direct recombination of photochemical reaction products, corrosion of Ag by an oxidant in the electrolyte, and electrode impedance and polarization effects are the main current limiting factors.

APPENDIX A

CYCLIC PHOTOGALVANIC SILVER HALIDE CELLS

INTRODUCTION

A. Photogalvanic Quantum Yield Studies

Since Becquerel¹ first discovered the photogalvanic effect, hundreds of papers on the subject appeared in the scientific literature.^{2,3} However most of these have dealt with open-circuit photopotentials rather than photocurrents. Although the former can offer interesting clues as to the type of photochemical products formed, if any, it is still essential for any practical photogalvanic cells and also for any thorough understanding of the kinetics of the photogalvanic process to obtain values of (a) the quantum yields of the individual photochemical reaction steps and (b) the net yields of the current that can be delivered for a given light input. Whereas the latter yields have been easily determined for dry photovoltaic cells such as the Si solar cells, there exist difficulties in measuring them in most photogalvanic systems.

To appreciate these difficulties it is necessary to distinguish at this point between those systems which in the dark: a) are in or near a thermodynamic equilibrium and in which the light either gives rise directly to products dischargeable through a battery circuit or else generates an e.m.f. capable of producing chemical changes by electrolysis; and those which b) are not in true thermodynamic equilibrium and in which the light catalyzes an otherwise extremely sluggish reaction or else accelerates the discharge of a battery by a photoconductive and/or depolarizing effect. Unfortunately, the systems for which photocurrent measurements have been reported seem to fall into group (b).^{4,5,6} Furthermore, the term photocurrent (defined as the increase in current delivered by a cell when the potential of the illuminated electrode is returned to the value in the dark by applying or adjusting an external voltage^{4,5}) does not distinguish between current generated by a photovoltage and that due to photoconductivity.

Let us consider for example a battery having an open circuit e.m.f. E_d in the dark and which comprises one electrode covered by a photosensitive material which also forms a current-limiting layer having a very high resistance R_d . When this electrode is illuminated, the current may increase from the value in the dark

$$I_d \approx E_d/R_d \quad (1)$$

to a much higher value

$$I_l \approx E_d/R_l \quad (2)$$

in light, due solely to a photoconductive effect. Now, it is known that photoconductors can have gains higher than one,⁷ i.e. one photon of light may allow passage of hundreds of electrons when an electric field is applied across the photoconductor. Thus one may obtain

deceptively high values for the photogalvanic quantum yields with batteries which would normally deliver a current in the dark, no matter how small (either spontaneously or with the aid of an external polarizing voltage), having the same polarity as the observed photocurrent.

Equations (1) and (2) describe essentially a conversion of chemical into electrical energy accelerated by light. If the term catalysis is generalized to include every type of acceleration of electrode discharge reactions, then equations (1) and (2) can be considered as describing a special form of the photocatalytic effect, and the current I_1 can be considered as a "photocatalytic" rather than "photogalvanic" current. This objection seems to apply to the few reported photocurrent measurements in electrolytic systems.⁴⁻⁶

On the other hand, in systems of group (a) the dark current I_d may again be described by equation (1); however, its low value must be associated with a low value of E_d rather than with a high R_d . The current could then increase to a higher value

$$I_1 \approx E_1/R_d \quad (3)$$

due to a photo-generated e.m.f. Since the latter implies actual conversion of light into electrical energy, equation (3) describes a truly photogalvanic current.

In frequent cases, however, both the e.m.f. and the resistance may change with illumination so that

$$I_1 \approx E_1/R_1 \quad (4)$$

The distinction between the photoconductive and the truly photogalvanic effects may then pose a problem. Of course, when E_1 is of opposite polarity than E_d , then I_1 must represent a truly photogalvanic current regardless of the value of R_1 . However, even in batteries having an e.m.f. in the dark of the same sign as in light it should be possible, in principle, to measure truly photogalvanic currents by a method of exhaustion, i.e. by starting with a very limited quantity of reducible and/or oxidizable components and drawing much more current over a long period of time than could have been delivered by complete discharge with 100% current efficiency. Obviously, the method of exhaustion will be most sensitive when a battery can be completely discharged at the start of the illumination or, what is tantamount but simpler, when the battery is assembled with the discharge products replacing at least one essential but missing reactant.

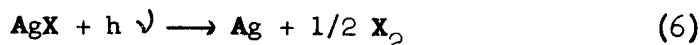
If a completely discharged battery can deliver appreciable current upon illumination, then the light apparently effects at least a partial regeneration of the battery reactants. These regenerated reactants thus undergo cyclic chemical changes.

In the present work, the photogalvanic quantum yield Y_p is defined as the ratio of the number of electrons N_e caused to go around an external circuit per number of absorbed photons N_{ph} in a cyclic photogalvanic cell.

$$Y_p = (N_e/N_{ph})_{\text{cyclic}} \quad (5)$$

For the most unambiguous measurements, the cell should have an initial open circuit voltage in the dark close to zero or possibly even of a sign opposite to that observed upon illumination. It is not necessary that the cell voltage reverse or disappear when illumination is discontinued. In fact, it is preferable for the cell to have a certain ability to store the charge and e.m.f. generated by the light. However, one of the criteria for a truly light-induced current is a marked increase of e.m.f. from a negligibly low value or complete reversal of polarity upon illumination of the initially assembled cell.

A review of previously reported truly photogalvanic systems suggests that the photogalvanic currents are usually both transient and extremely low (i.e., less than μA) because of the absence of provisions for effective cyclic utilization and regeneration of reaction products. For instance, Becquerel's photogalvanic cells¹ consisted essentially of one bare Pt electrode and one Pt electrode covered with AgX ($\text{X} = \text{I}, \text{Br}$ or Cl) both immersed in the same electrolyte solution. However, the halogen formed in the photochemical reaction



cannot diffuse to the bare Pt electrode at a sufficiently high rate to give rise to appreciable electrode discharge reactions, because appreciable diffusion of the X_2 would require a rather high concentration of X_2 near the AgX . This would be difficult (if not impossible) to achieve by illumination on account of the tendency for the X_2 to recombine with the photolytically formed Ag.

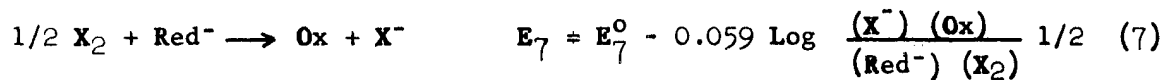
The present studies are aimed at the development of cyclic photogalvanic cells and of methods of maximizing the quantum yield Y_p . A preliminary survey² led to the choice of photogalvanic cells based on reaction (6).

B. Cyclic Silver Halide Photogalvanic Cells

a) Photochemical Charging and Discharging Reactions (Figures 1 and 2)

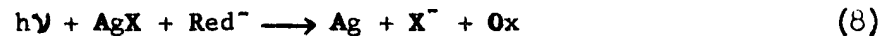
In the present work (see Figure 1), the cells differ from the Becquerel cell in that they contain in addition the components Red^- and

Ox of a suitable reduction-oxidation couple which can remove the X_2 at the AgX-electrolyte interface via the reaction



where the symbols in parentheses represent the concentrations of the respective components.

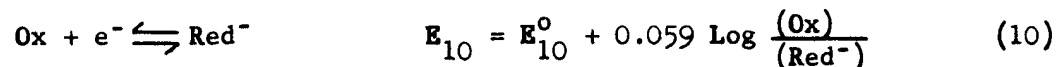
The net result of reactions (6) and (7) is then



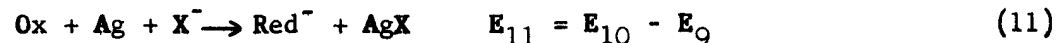
which can be considered as a photochemical recharging of an Ag-Ox battery completely discharged via the reactions



and

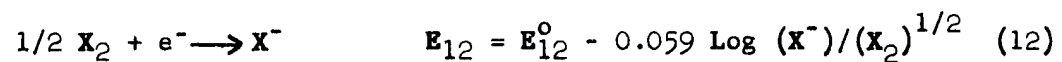


yielding an overall discharge reaction



which is the reverse of reaction (8).

In order for the cell to be cyclic, the discharge reaction should occur spontaneously; i.e., E_{11} should be positive. Furthermore, in order for reaction (7) to occur, it is necessary that the potential E_{12} for the reaction



be higher than E_{10} . Hence

$$E_9 < E_{10} < E_{12} \quad (13)$$

which is a basic limitation on the choice of the $\text{Red}^- - \text{Ox}$ couple.

b) Competing Wasteful Reactions (Figure 3)

Reaction (6) can be considered to be composed of the basic electronic process



□

where e^- and h^+ are electrons and holes, respectively, followed by



and



as shown in Figure 2

This suggests the possibility of several wasteful recombination reactions shown in Figure 3



or, what is more likely,



followed by

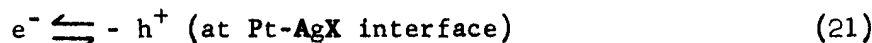


where R , R^- may be an impurity or lattice defect acting as a center for the recombination of holes with electrons.

On the other hand, the useful discharge reaction step (9) can also be regarded as the sum of



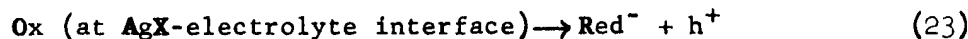
and




where the h^+ originates at the Pt electrode as shown in Figure 2. The last two steps must be differentiated on the one hand from the following wasteful reactions shown in Figure 3



or



followed by reaction (22), where the h^+ originates from reaction (14) or (23), and on the other hand from the sequence of reactions (10), (20), and (21) all occurring at the Pt-AgCl electrode in case of porosity of the AgX film, as shown at the bottom of Figure 3. All these wasteful reactions represent short-circuiting paths for the recombination of e^- with h^+ without passage of the e^- through an external circuit.



c) Other Current-Limiting Factors

Even in the absence of the above parasitic reaction mechanisms, the current-density is limited by the resistance across the AgX film and by concentration and electrode polarization effects.

Attempts to reduce these limitations introduces other difficulties. E.g., thinner films of AgX will have lower resistance, but they also form the short-circuiting pores considered in the preceding section. Furthermore, an appreciable fraction of the useful radiation of wavelengths approximating the absorption edge of the AgX may be lost by the thinner films but absorbed and converted into useful currents by the thicker ones. Similarly, concentration polarization effects are reduced with high (Ox) concentrations, but these accelerate the parasitic reaction (23).

C. Experimental Procedure

a) Optical System

The optical arrangement is shown schematically in Figure 4. Light from a 30-watt microscope lamp having a color temperature of 2400 to 2700°K was focused onto an area of 1 to 2 cm² of the Pt-AgX electrode g by means of the hemispherical mirror m and the condensing lens C. Most of the infrared radiation was absorbed by the water filter W. Filters B and D could be of the narrow-band interference type for experiments with monochromatic radiation, neutral density filters for studies with varying light intensities, or Wratten filters for cutting out some of the longer or shorter wavelength components in special orienting experiments.

Relative light intensity measurements were performed with the photocell P located behind the transparent cell E. Absolute light intensity measurements were obtained by focusing the light source on a previously calibrated photovoltaic Si cell about 1 x 2 cm² in area (not shown in Figure 4).

b) Test Cell Assembly

The test cell E was a square transparent Lucite box with an outer jacket containing circulating water from a thermostat bath at 25°C. Electrode f was a 52 mesh Pt gauze made of 0.004-inch diameter wire, transmitting about 60 to 70% of the impinging radiation. Electrode g was prepared by abrading the surface of a 0.002-inch thick Pt foil with grade 320 emery paper, etching in aqua regia, rinsing, immersing in molten AgX contained in a porcelain crucible at about 500°C and slowly withdrawing the Pt while allowing the edge of the Pt to touch the crucible.

The resulting films of AgX over the Pt surface were well-adhering, about 5-20 microns thick, and impervious to the electrolyte. The latter consisted of solutions of 0.001 to 0.1 (usually 0.01) M FeCl₂ plus 0.01 to

1 (usually 0.2) M HCl in experiments with Pt-AgCl electrodes, and of 0.01 M NaBr plus 0.005 M FeSO₄ with Pt-AgBr. The ratio of Fe⁺² to Fe⁺³ ions was maintained nearly constant in some experiments by addition of FeCl₃ complexed with an excess of HF.

All reagents were of analytical grade. The AgCl was Baker Analyzed reagent, whereas the AgBr was prepared by precipitation of 0.2 M AgNO₃ solutions with either 0.2 M NaBr or 0.2 M HBr.

c) Electrical Measurements

A model 153 X 12V-X-6 25-mv Brown potentiometer recorded the voltage drop across one of two resistance boxes connected in series with the test cell electrodes f and g of Figure 4. Current-sensitivity and total external resistance could be adjusted at will by means of the two resistance boxes.

Internal cell resistances were not measured by means of the usual alternating current bridge method, in order to remove the possibility of any net charging effects resulting from the application of an external alternating voltage. Instead, the internal cell resistances were deduced from a series of current measurements with varying external resistances in the high external resistance range, where the current output was low enough to eliminate polarization effects. The same measurements also yielded the values of open circuit cell voltage, which agreed with readings of a 10-megohm vacuum-type voltmeter. On the other hand, the quantum yield measurements usually involved relatively low external resistances.

d) Photochemical Quantum Yield Measurements

The yields of reaction (3) were also measured by purely chemical methods. A beaker containing a stirred mixture of 4 Gm powdered AgX and 100 cc of 0.001M FeX₂ plus 0.02M HX was illuminated with the above mentioned 30-watt microscope lamp for 1-to-10 minute intervals. The powder was then allowed to settle and 10-cc samples of the solution were withdrawn and analyzed for Fe⁺² ions by a permanganometric method.⁹ Control titrations were also performed on samples from mixtures stirred in the dark and from illuminated mixtures of 4 Gm. Cr₂O₃ with the same solution, to correct for any air-oxidation of Fe⁺² ions. The rates of conversion of Fe⁺² to Fe⁺³ ions in the control experiments were negligibly low in comparison with those observed upon illumination of the AgX.

EXPERIMENTAL RESULTS

The discharge characteristics of a typical Pt-AgCl, FeCl₂, Pt cell are shown in Figure 5. Upon illumination of the Pt-AgCl electrodes in initially assembled test cells, the open-circuit e.m.f. rose from values of less than 50 mv to a value of about 0.4 v corresponding to the e.m.f.

of an Ag-AgCl-FeCl₃-Pt battery. This satisfies, then, one basic criterion enounced near the end of Section I.A. Furthermore, the slow continuous rise in current and voltage over a period of more than 10 minutes indicates a gradual build-up of photochemical reaction products. Finally, a most convincing proof of true photochemical charging was obtained by illuminating the cells for varying time intervals while on open-circuit and integrating the total current that could be withdrawn in the dark immediately following the illumination, as shown in Figure 6. The plot of charge withdrawn versus time of illumination is linear (Figure 7), in agreement with the charging reaction of Section I.B. (a).

The electrodes used for the results of Figure 7 were among the earliest and least efficient ones, yielding an average current of less than 10 μ A during continuous illumination. In order to optimize the current yields, the thickness of the AgCl-layers and composition of the solution were varied. Using a 1/100 M solution of FeCl₂ which was approximately 1/1000 molar in FeCl₃, charging currents of up to 80 μ A for a short period of time and up to 40 μ A for several hours were obtained, when the AgCl-layers were 5-20 microns thick.

With thinner layers, higher porosity and lower light absorption led to a lower efficiency whereas with thick layers (> 20 μ) the high impedance of the Pt-AgCl electrode limits the current.

The best results obtained correspond to quantum yields of 2 to 5% for light of wavelengths shorter than 4,000 Å. The relative sensitivity of two Pt-AgCl electrodes to various wavelengths is shown in Figure 8.

By varying the intensity of illumination with neutral density filters, it was found that the current yield increased linearly with intensity (Figure 9), showing no sign of any intensity saturation effect with the light source used.

With Pt-AgBr electrodes the voltage and current changes upon illumination were small and usually in a direction opposite to that expected by the reaction scheme of Section I.B. (a), when the AgBr was prepared from NaBr and AgNO₃ solutions. However, with AgBr prepared from HBr and AgNO₃ solutions, both the polarity of the photo-induced voltage and the photogalvanic quantum yields were comparable to those obtained with AgCl. Furthermore, since the fraction of light from tungsten at 2600°K absorbed by AgBr is about four times larger than the fraction absorbed by AgCl, the actual photogalvanic currents with the same illumination were correspondingly increased by a factor of three to four. With monochromatic light of various wavelengths, the relative photogalvanic quantum yields varied as shown in Figure 10.

When exposed to the white light of a microscope lamp the AgBr electrodes showed a change of color and a simultaneous decrease in photogalvanic efficiency within a few hours. It is known¹⁰ that light of wave-

lengths longer than the absorption edge may disperse the photolytically formed Ag forming an Ag colloid with an absorption band extending into the intrinsic absorption region of the AgX. This colloid may decrease the amount of light available for photolytically active absorption. Furthermore, the colloidal Ag may accelerate hole-electron recombination via the reaction steps (15) and (22). (Cf. Figure 3 section I.B. (b).)

This possibility was partly confirmed with filtered light in the range of 3300-4400 Å was used for illumination of the AgBr. Almost no color change could be observed under steady state conditions and the photolytic sensitivity of the electrodes decreased only after a few days, this decrease being probably due to the formation of pores.

It is noteworthy that the spectral sensitivity curves for both AgCl and AgBr (Figures 8 and 10) show maximum quantum yields for wavelengths just below the absorption edges of the respective halides. To explain the decrease in quantum yield with decreasing wavelengths one may assume that the latter, being highly absorbed at the very surface of the AgX, result in the formation of Ag near the AgX-electrolyte interface where re-oxidation by Fe^{+3} ions is relatively fast. Evidence for this kind of recombination is given in Figures 11 and 12. In Figure 11, 80% of the charge formed by illumination of a Pt-AgCl, $FeCl_2$, Pt cell for 8.5 minutes is shown to disappear within 20 minutes. In Figure 12, the photogalvanic current is found to be inversely proportional to the Fe^{+3} ion concentration, for concentrations above 10^{-4} M $FeCl_3$.

Whereas the photogalvanic quantum yields were usually less than 5% with both Pt-AgCl and Pt-AgBr electrodes, the photochemical quantum yields for the conversion of Fe^{+2} to Fe^{+3} ions by illumination of both AgCl and AgBr powders (cf. section I. C. (d)) were 50-100%. These high yields may be attributed partly to the absence of the stringent electrochemical requirements for the delivery of useful photogalvanic currents and partly to the large effective surface area of the powdered AgX with a corresponding low surface density of photochemically formed Ag taking part in wasteful recombination reactions.

CONCLUSIONS

Partial photochemical charging of a Pt-Ag-AgX, aqueous FeX_3 , Pt cells was achieved with maximum photogalvanic quantum yields of 2 to 5% in cells remaining in a state of nearly complete discharge.

In partly charged batteries, i.e. containing more than 10^{-4} M FeX_3 or an appreciable surface concentration of Ag, direct attack of the Ag by Fe^{+3} ions appreciably reduces the photogalvanic quantum yields in direct proportion to the Fe^{+3} ion concentration. When the latter reaches or exceeds 0.001M, the quantum yield may be reduced by a factor

25X1

of ten or more. On the other hand, for Fe^{+3} ion concentrations below 10^{-4}M the photogalvanic current is severely limited by concentration polarization at the Pt- FeX_3 electrode. The optimum Fe^{+3} ion concentration is therefore limited to the fairly narrow range of 10^{-3} to 10^{-4}M .

However, the most serious drawback of these cells is the deterioration observed after 1 to 5 days of illumination, attributable mainly to the development of pores in the AgX film (cf. Figure 3, Section I. B. (b)).

Whereas the last difficulty applies only to AgX-covered Pt electrodes, the problem of diffusion-limited current with low photochemical product concentrations and of recombination with higher concentrations is likely to be encountered in most photogalvanic systems. Some approaches towards a solution of this problem are presented in a following publication.


ACKNOWLEDGEMENTS

25X1

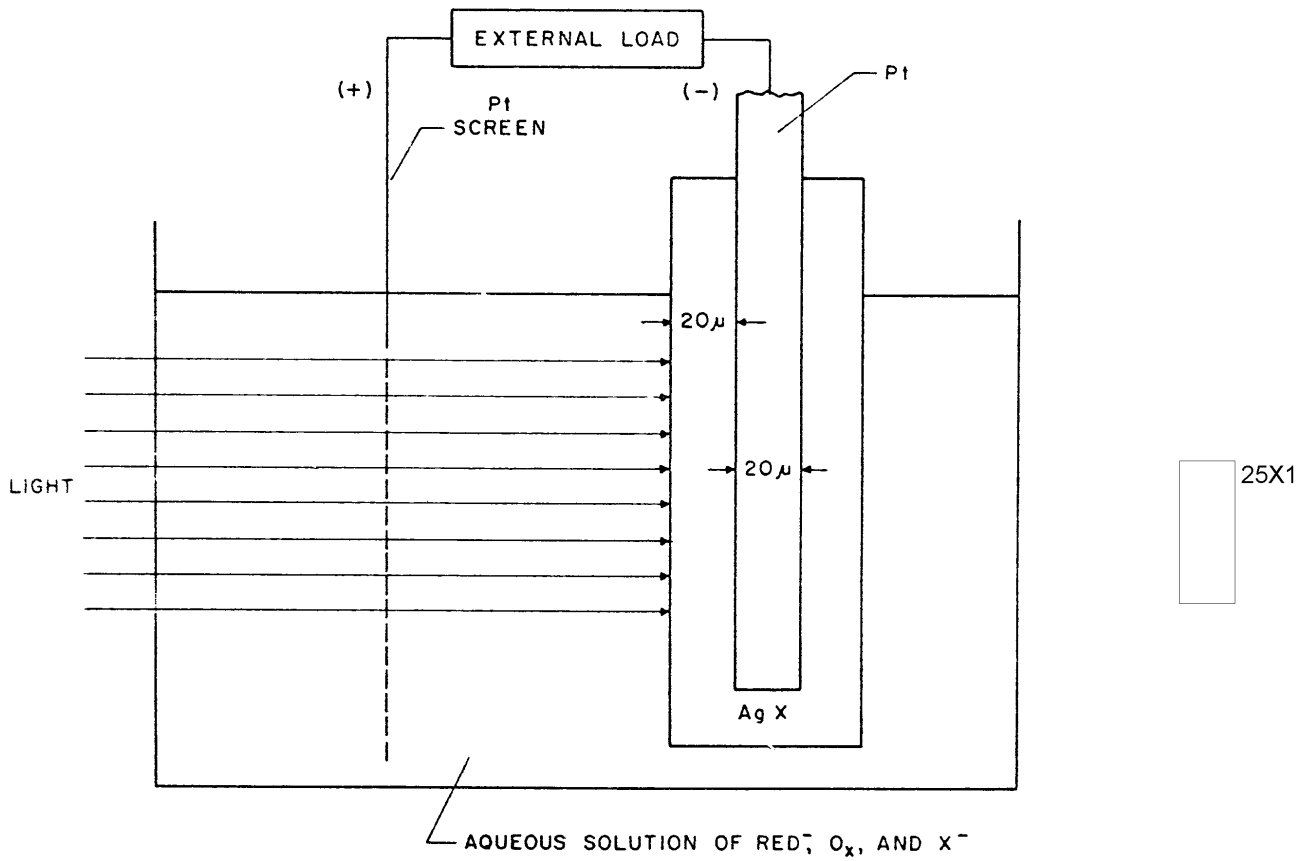
25X1



REFERENCES

1. E. Becquerel, Compt. rend. 9, 561 (1839)
2. A. W. Copeland, O. D. Black, and A. B. Garrett, Chem. Rev. 31, 177, (1942)
3. K. M. Sancier, Trans. Conf. Use of Solar Energy (University of Arizona Press, 1958) V, pp. 43-56
4. H. Luggin. Z. Physik. Chem., 23, 577 (1897)
5. V. I. Veselovsky, J. Phys. Chem. (U.S.S.R.) 22, 1302 (1948)
6. A. Goldman and J. Brodsky, Ann. Physik, 44, 849 (1914); C. G. Fink and D. K. Adler, Trans. Am. Electrochem. Soc. 58, 175 (1930)
7. A. Rose, Proc. I. R. E. 43, 1850 (1955)
8. 
9. I. M. Kolthoff and E. B. Sandell, Textbook of Quantitative Inorganic Analysis (Macmillan, New York, 1946) pp. 592
10. C. E. K. Mees, The Theory of the Photographic Process (Macmillan, New York, 1946) pp. 285 ff.

25X1



A-12

FIGURE 1 Schematic Drawing of a Cyclic Silver Halide Photogalvanic Cell

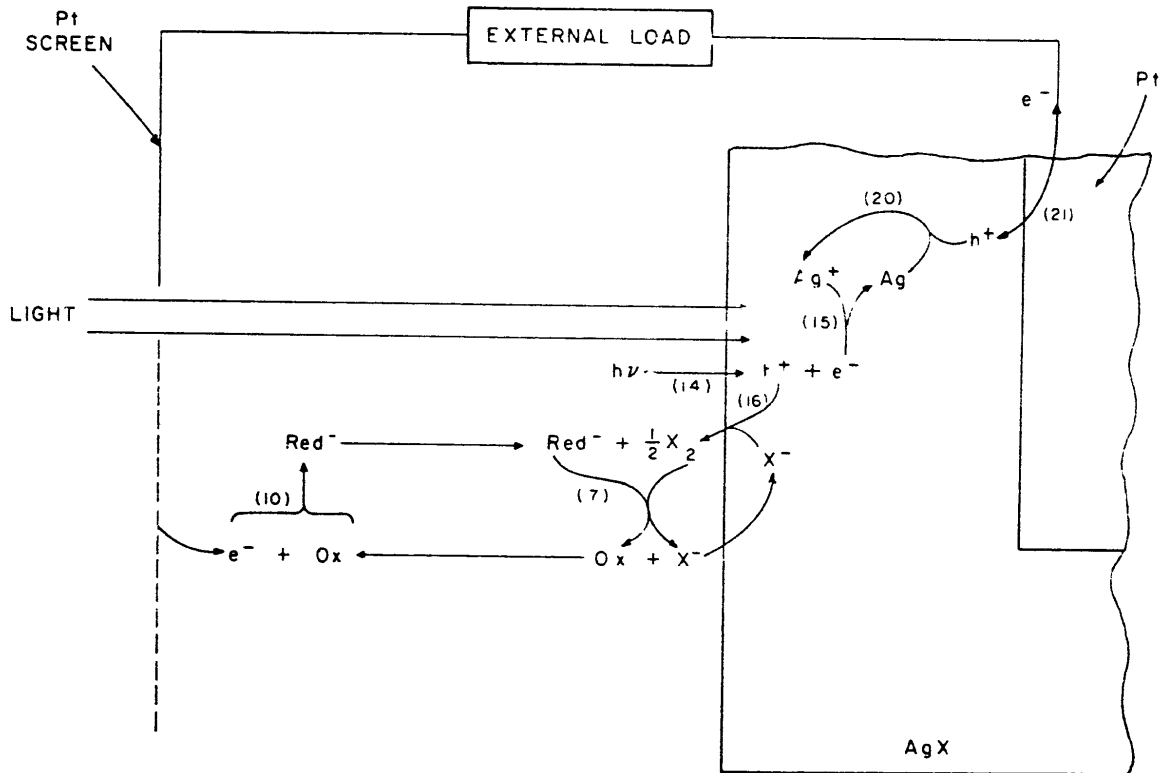


FIGURE 2 Discharging and Photochemical Charging Reactions at the Electrodes of the Cell of Figure 1

A-13

25X1

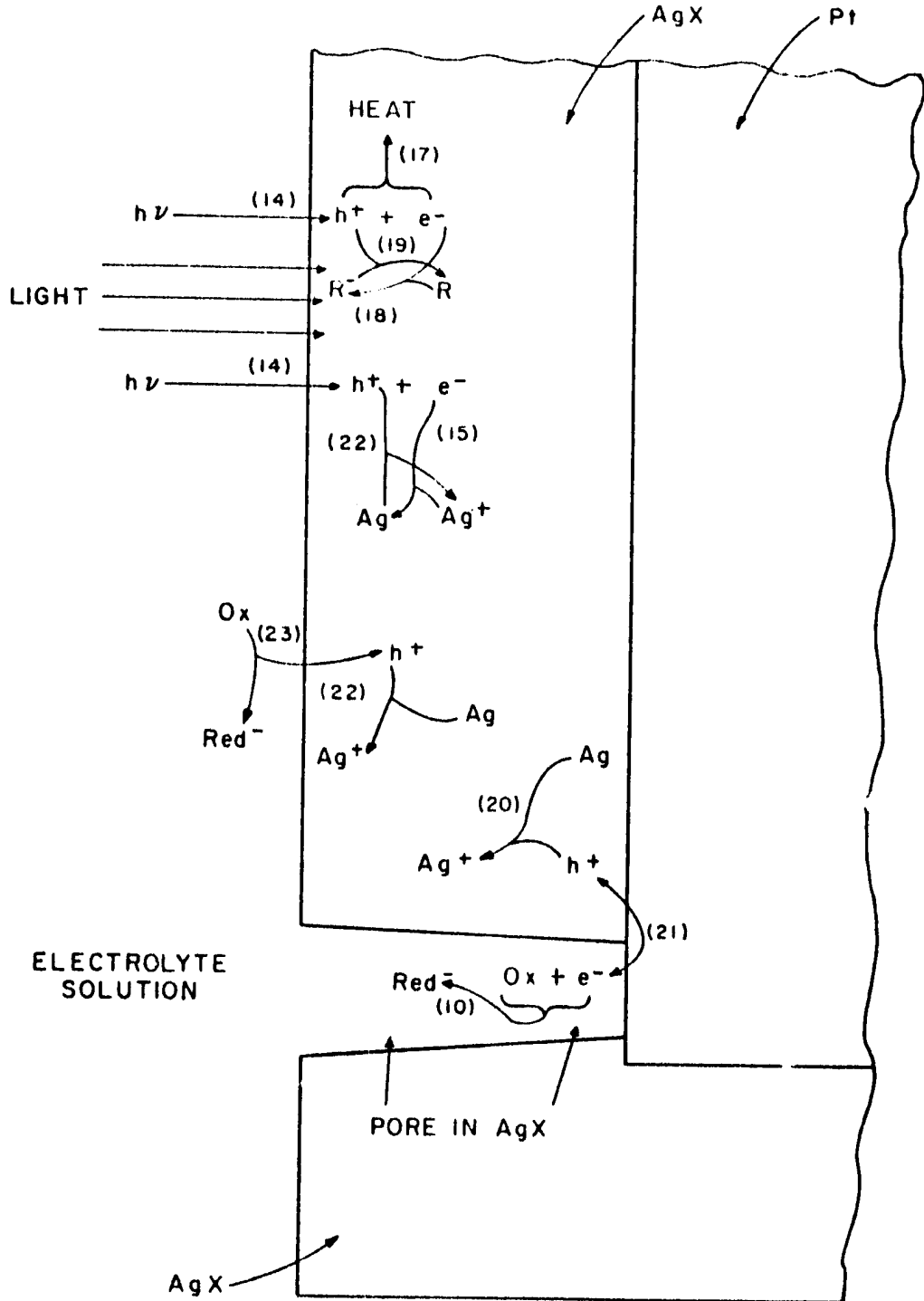
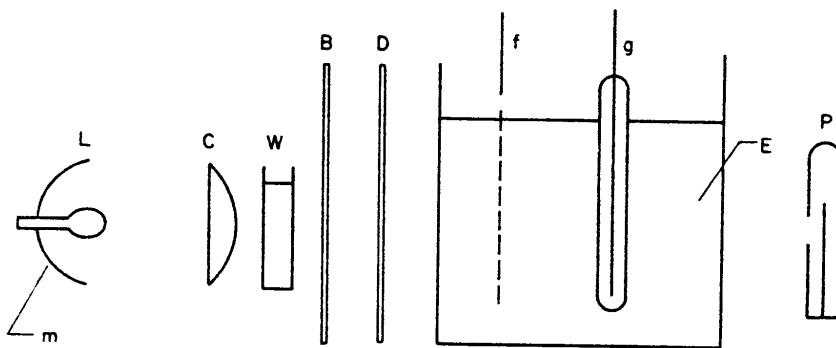


FIGURE 3 Wasteful Recombination Mechanisms at the Pt-AgX Electrode of Figure 1



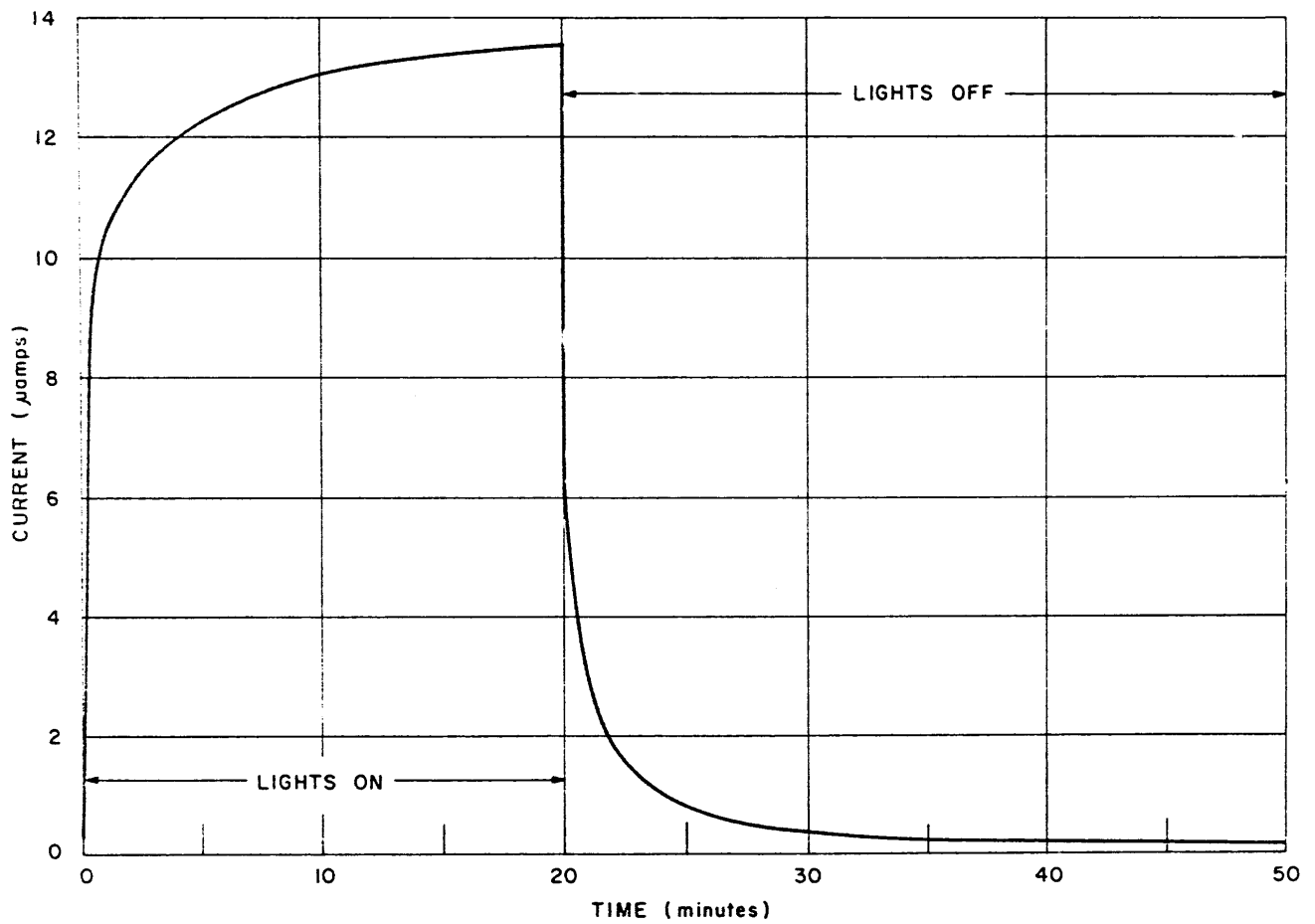
25X1



A-15

FIGURE 4 Optical Systems for Photogalvanic Quantum Yield Measurements. Light from the 30-watt microscope lamp L is focused by means of the adjustable reflecting mirror m and condensing lens C onto the Pt-AgX electrode g. Intensity and composition of the light are adjusted by means of the water filter W and interchangeable filters B and D. Phototube P located behind the test cell E measures relative light intensities when the electrodes f and g are temporarily removed.

A-16



25X1



FIGURE 5 Typical Changes of Current Delivered by a Pt-AgCl, FeCl₂, Pt Cell with and without Illumination

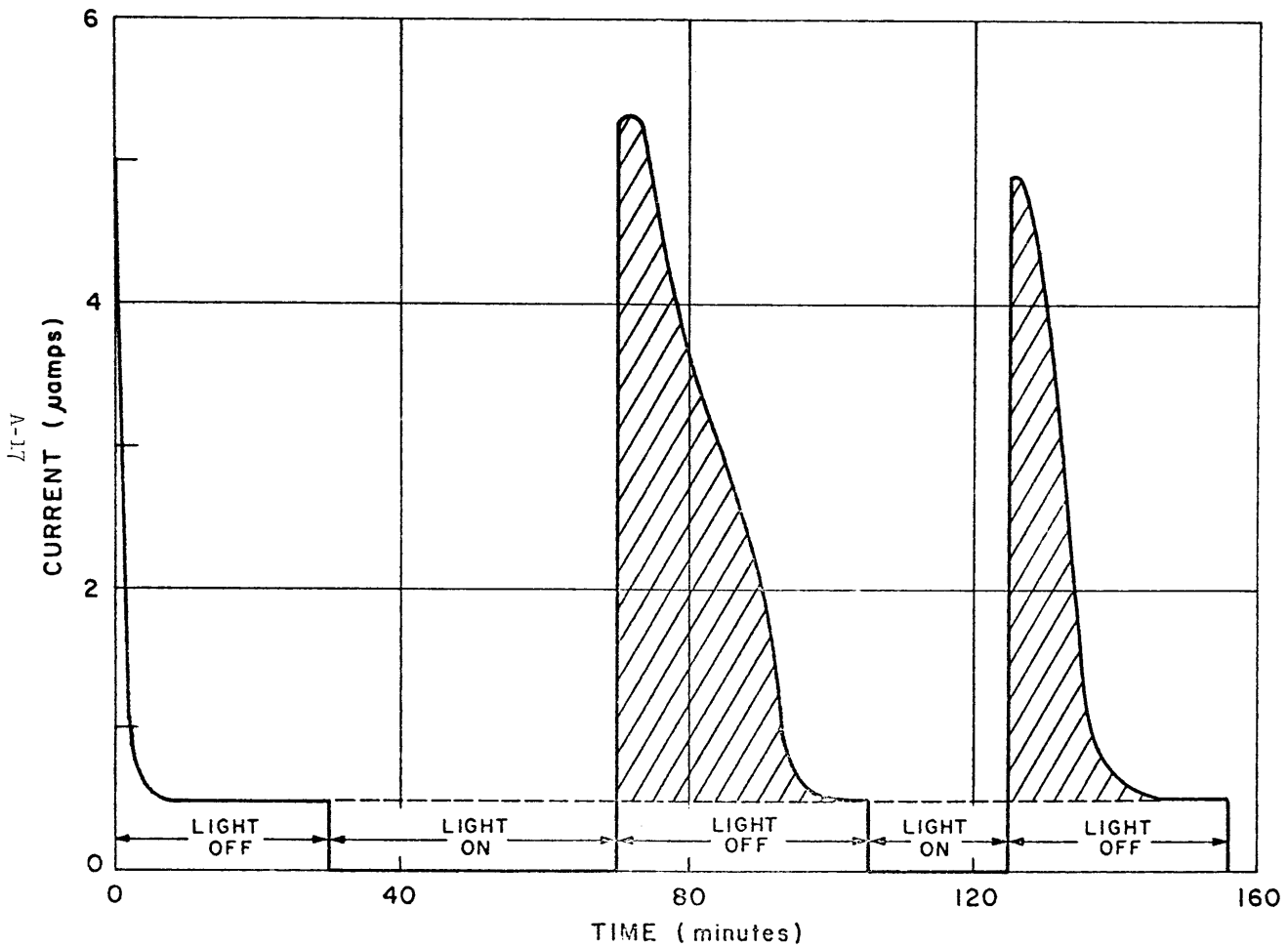


FIGURE 6 Current Withdrawn in the Dark from a Pt-AgCl, FeCl₂, Pt Cell Following Different Periods of Illumination
Declassified in Part - Sanitized Copy Approved for Release 2012/02/16 : CIA-RDP78-03424A001200030004-3

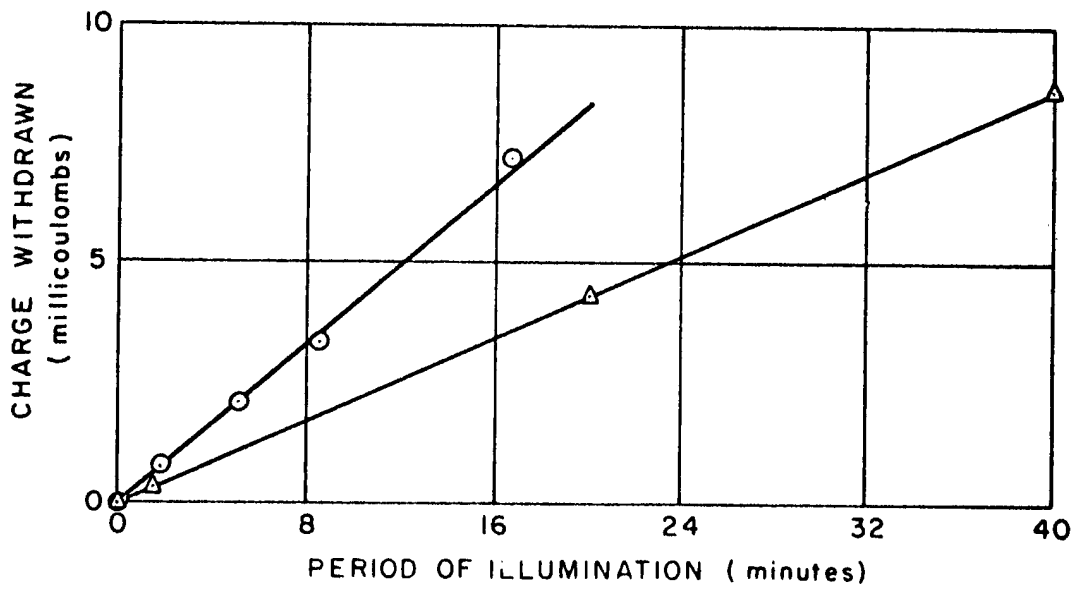


FIGURE 7 Charge Withdrawn from Two Different Pt-AgCl Electrodes After Various Periods of Illumination

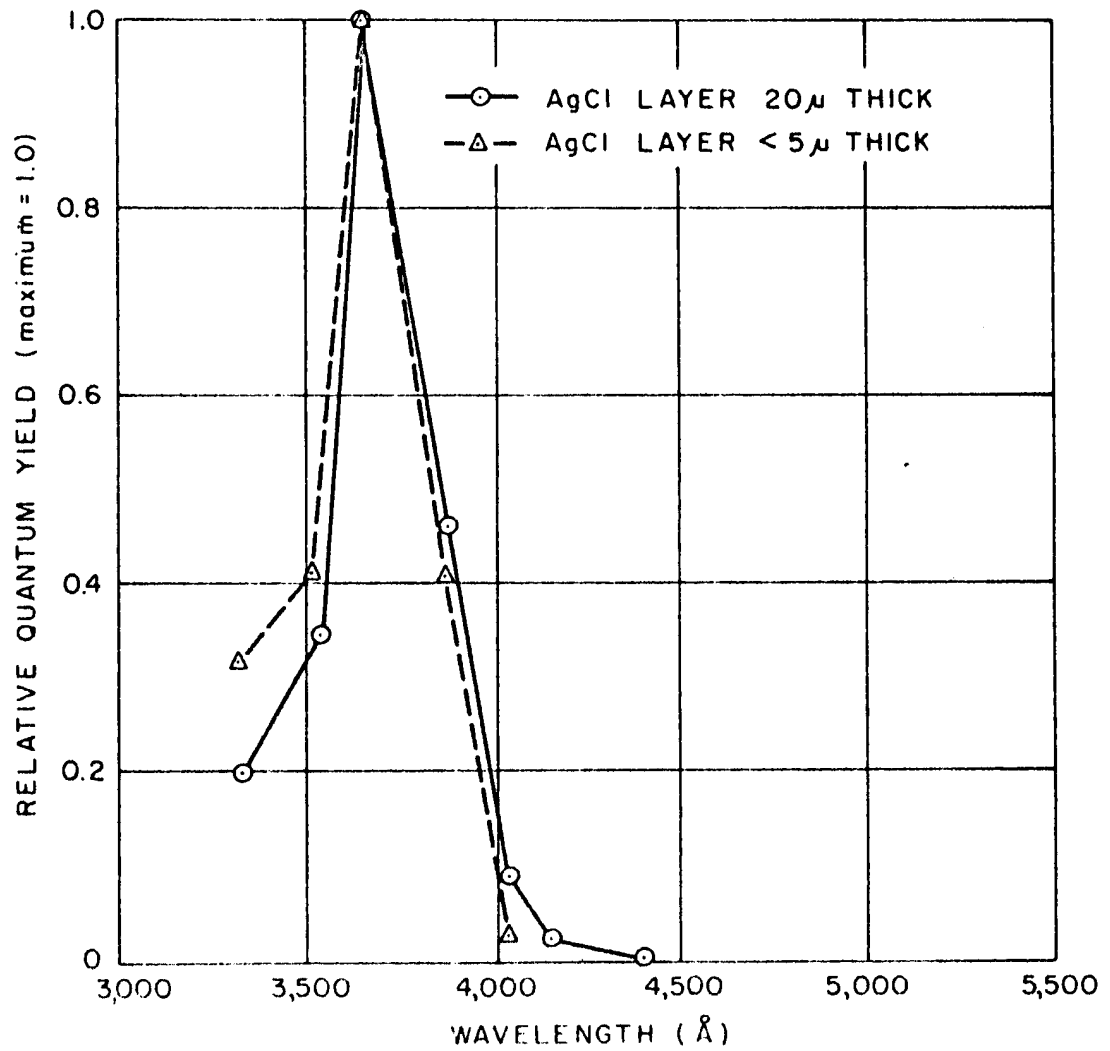


FIGURE 8 Relative Dependence of the Photogalvanic Quantum Yield from Pt-AgCl Electrodes on Wavelength

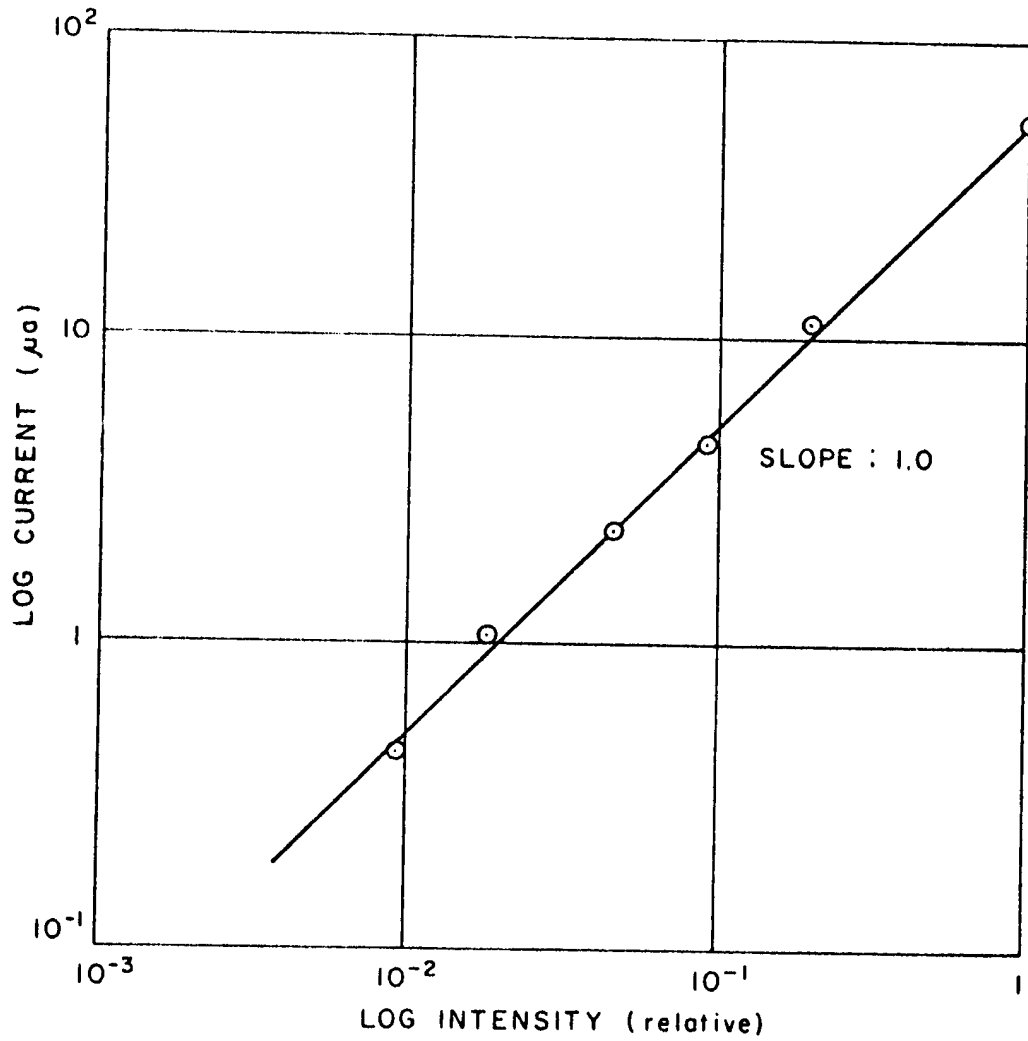


FIGURE 9(a) Logarithmic Plot

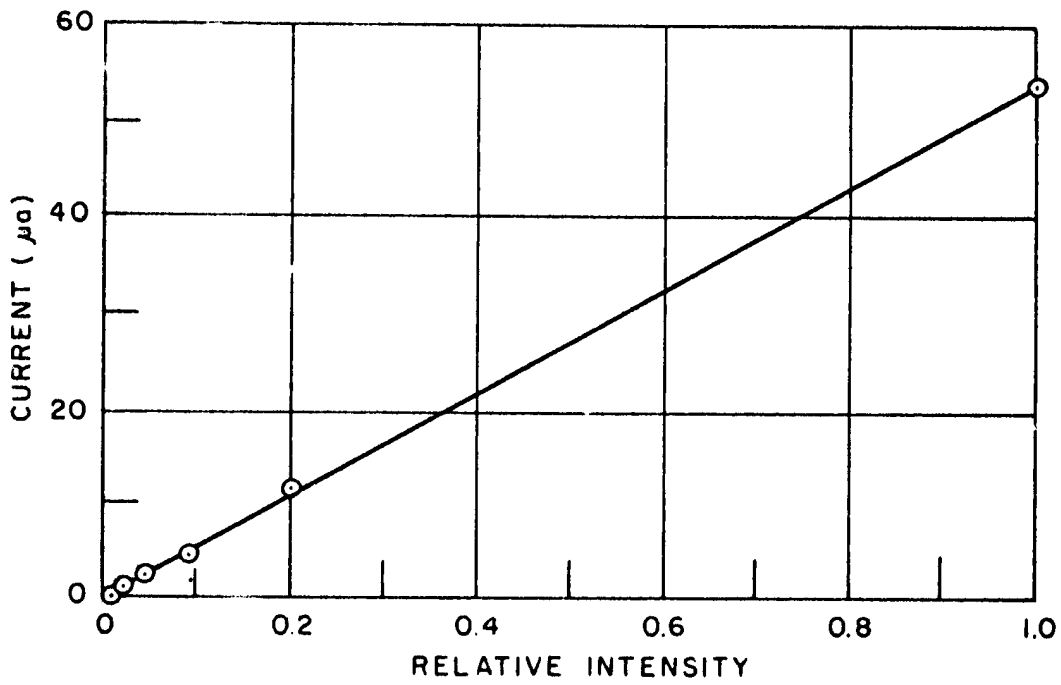


FIGURE 9(b) Linear Plot

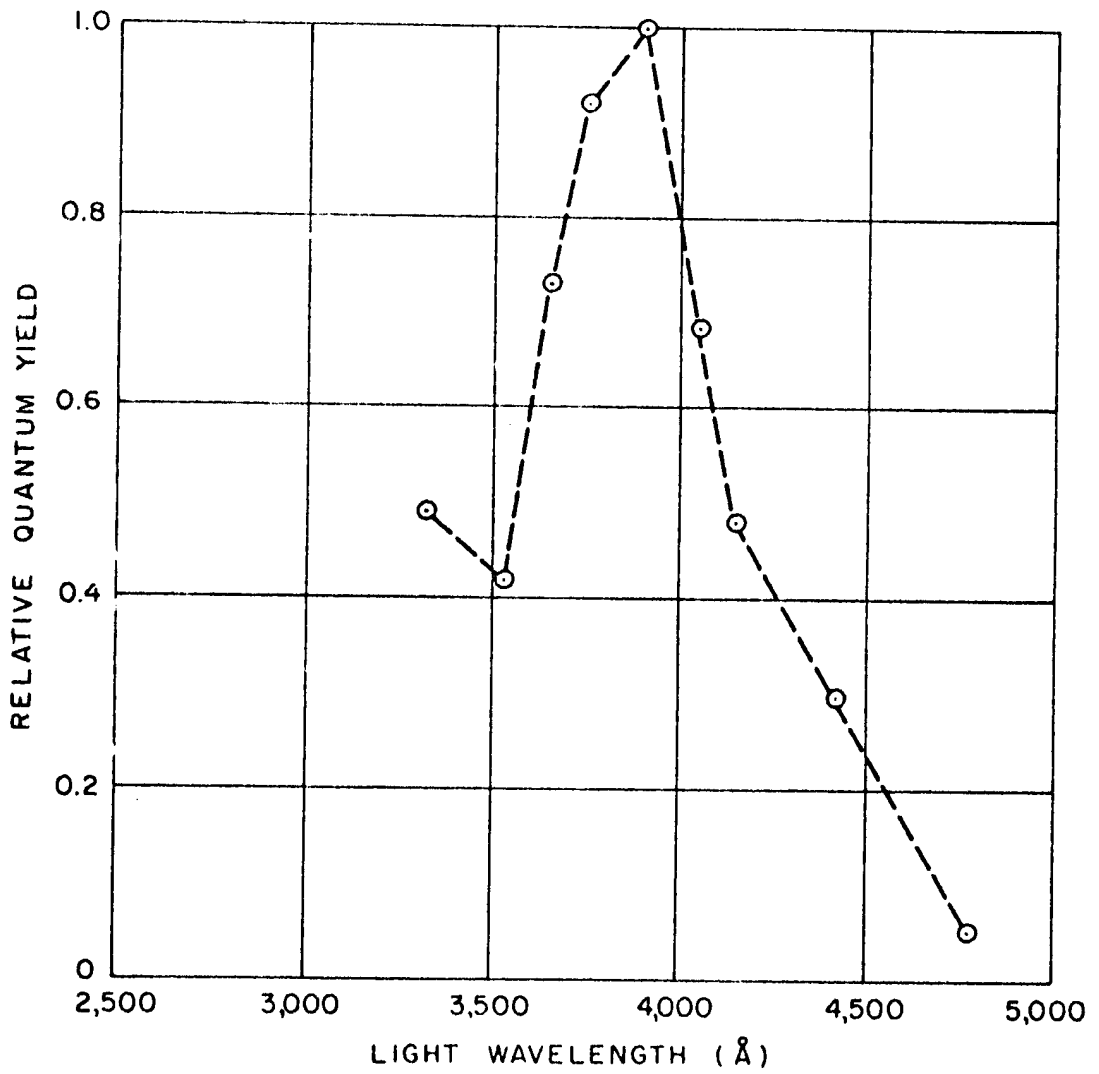
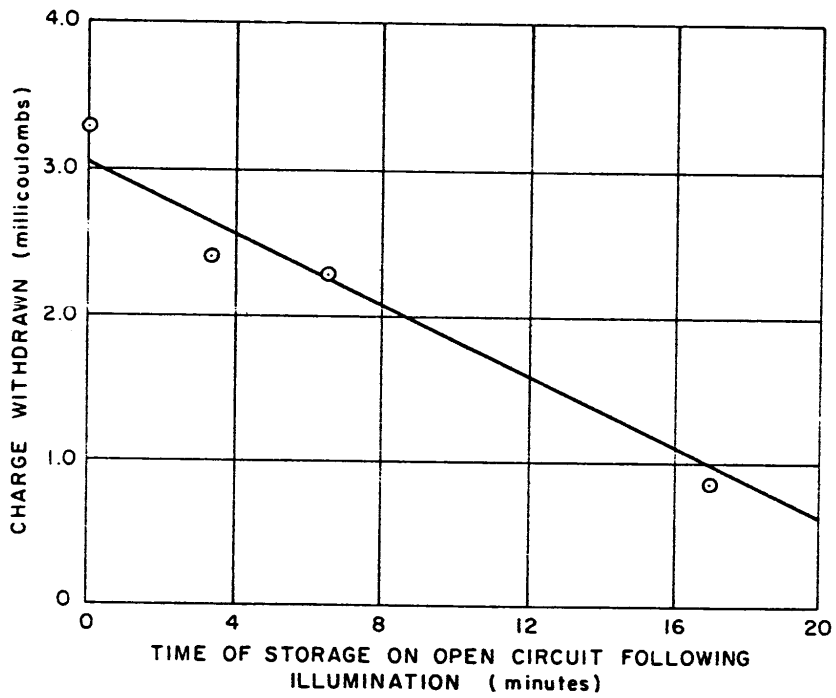


FIGURE 10 Relative Photogalvanic Quantum Yields from Pt-AgBr Electrodes with Light of Various Wavelengths



25X1



A-23

FIGURE 11 Loss of Charge During Open Circuit Storage

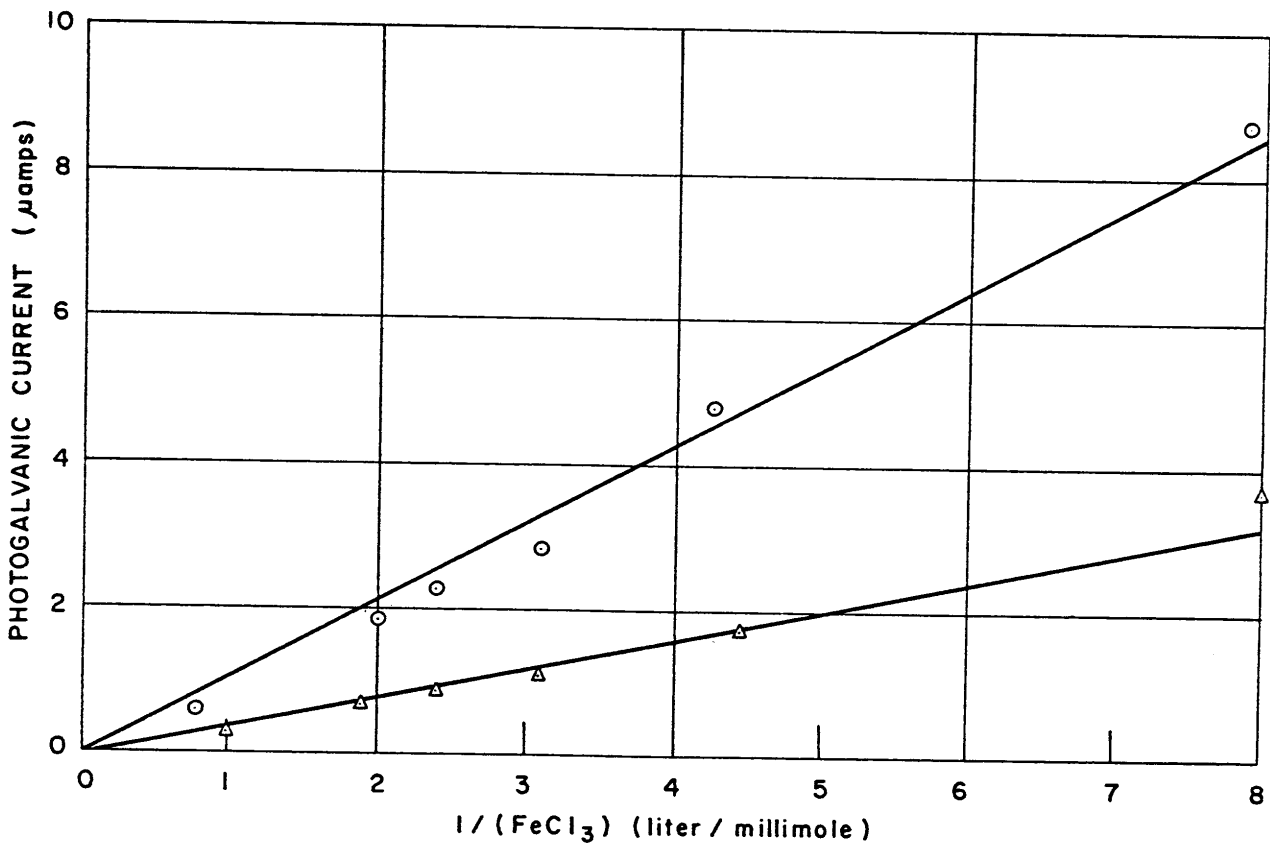


FIGURE 12 Inverse Proportionality of Photogalvanic Current to the FeCl_3 Concentration Observed with Two Pt-AgCl Electrodes

CONFIDENTIAL A-24



25X1

CONFIDENTIAL